

# Opposite effects of aerosols and meteorological parameters on warm clouds in two contrasting regions over eastern China

5 Yuqin Liu<sup>1,4</sup>, Tao Lin<sup>1,4</sup>, Jiahua Zhang<sup>2</sup>, Fu Wang<sup>3</sup>, Yiyi Huang<sup>1</sup>, Xian Wu<sup>1</sup>, Hong Ye<sup>1</sup>, Guoqin Zhang<sup>1</sup>,  
Xin Cao<sup>1,4</sup>, Gerrit de Leeuw<sup>5,6</sup>

1 Key Lab of Urban Environment and Health, Institute of Urban Environment, Chinese Academy of Sciences, Xiamen 361021, China

2 Key Laboratory of Digital Earth Sciences, The Aerospace Information Research Institute, Chinese Academy of Sciences, Beijing 100094, China

3 CMA Earth System Modeling and Prediction Centre (CEMC), Beijing 100081, China

10 4 Fujian Key Laboratory of Digital Technology for Territorial Space Analysis and Simulation, Fuzhou 350108, China

5 Royal Netherlands Meteorological Institute (KNMI), R&D Satellite Observations, 3730AE De Bilt, The Netherlands

6 Aerospace Information Research Institute, Chinese Academy of Sciences (AirCAS), [No.9 Dengzhuang South Road, Haidian District, Beijing 100094](#)~~No.20 Datun Road, Chaoyang District, Beijing 100101~~, China

*Correspondence to: Gerrit de Leeuw(gerrit.de.leeuw@knmi.nl), Tao Lin (tlin@iue.ac.cn)*

15

**Abstract.** ~~Most of previous studies addressed~~ The sensitivity (S) of cloud parameters to the influence of different aerosol and meteorological parameters on the sensitivity of cloud parameters to aerosol indirect effect has in most previous aerosol-cloud interaction (aci) studies been addressed using traditional statistical methods. In the current study, relationships between cloud droplet effective radius (CER) and aerosol optical depth (AOD, used as a proxy for aerosol concentration) cloud condensation nuclei, CCN<sub>c</sub> concentrations), characterized by i.e. the sensitivity (S) of CER to AOD (S<sub>CER-AOD</sub>), is investigated with were constructed for different constraints of AOD and cloud liquid water path (LWP). In addition to traditional statistical methods, The geographical detector method (GDM) is applied in this study to quantify the relative importance of the effects of aerosol and meteorological parameters, and their interaction, on S.

~~Aerosol and cloud properties retrieved from~~ The Moderate Resolution Imaging Spectroradiometer (MODIS) on board the Aqua satellite C6 L3 data and the European Centre for Medium-Range Weather Forecasts (ECMWF) ERA-5 reanalysis data, for the period from 2008 to 2022, were used to investigate ~~aerosol-cloud interaction (ACIaci)~~ aerosol-cloud interaction (ACIaci) over eastern China, ~~using aerosol optical depth (AOD) as a proxy for the aerosol concentration, during a period of 15 years (2008-2022).~~ Two contrasting areas were selected: the heavily polluted Yangtze River Delta (YRD) and a relatively clean area over the East China Sea (ECS). Linear regression analysis shows ~~that the opposite sensitivity (S) of behaviour of the cloud droplet effective radius (CER) to and AOD relationship in the two different aerosol regimes.~~ CER

20

25

30

decreases with the increase of AOD (negative S) in the moderately polluted atmosphere ( $0.1 < \text{AOD} < 0.3$ ) over the ECS, whereas, in contrast, ~~in agreement with the Twomey effect. However,~~ but CER increases  
35 with increasing AOD (positive S) in the polluted atmosphere ( $\text{AOD} > 0.3$ ) over the YRD, ~~CER increases~~  
with increasing AOD (positive S). Evaluation of ~~the ACI index (here defined as the change in CER as~~  
a function of AOD) as function of the ~~cloud liquid water path (LWP)~~ shows that in the moderately  
polluted atmosphere over the ECS, ~~the ACI index is significant and positive-negative~~ in the LWP  
interval [ $40 \text{ g m}^{-2}$ ,  $200 \text{ g m}^{-2}$ ], and the sensitivity of CER to AOD is increases substantially stronger as  
40 with LWP increasing LWP is larger. In contrast, in the polluted atmosphere over the YRD, ~~S the ACI~~  
index is significant and negative-positive in the LWP interval [ $0 \text{ g m}^{-2}$ ,  $120 \text{ g m}^{-2}$ ] and does not change  
notably as function of LWP in this interval. The study further shows that over the ECS the CER is larger  
for higher LTS and RH but lower for higher PVV. Over the YRD, there is no significant influence of  
LTS on the relationship between CER and AOD. Furthermore, ~~the GDM has been used as an~~  
45 independent method to ~~To further~~ analyse the sensitivity of cloud parameters to influence of AOD and  
meteorological ~~conditions~~ parameters (relative humidity, RH; lower tropospheric stability, LTS; and  
pressure vertical velocity, PVV on cloud parameters). The GDM has also been used to analyse the effects  
of interactions between two parameters and thus obtain information on confounding meteorological  
effects on the aci. ~~the geographical detector method (GDM) has been used. The results show that all~~  
50 factors have a significant influence on the cloud parameters ~~Over the ECS, cloud parameters are~~  
sensitive to almost of all parameters considered; except for cloud top pressure (CTP), ~~but and~~ the  
sensitivity to influence of AOD is larger than that of to any of the meteorological factors. Among the  
meteorological factors, ~~lower tropospheric stability (LTS) has the largest influence on~~ the cloud  
parameters are most sensitive to LTSPVV and least sensitive to relative humidity (RH) the smallest. Over  
55 the YRD, the explanatory power of the sensitivity of cloud parameters to effect of AOD and  
meteorological parameters ~~on cloud parameters~~ is much smaller than over the ECS, except for RH which  
has a statistically significant influence on CTP and can explain ~~65~~ 74% of the variation of CTP. The  
results from the GDM analysis show that the explanatory power of the combined effects of aerosol and  
a meteorological parameter is larger than that of each parameter alone. Thus, the GDM provides an  
60 alternative way to obtain information on confounding effects of different parameters. ~~The combined effect~~  
of meteorological factors and AOD on cloud parameters enhances the explanatory power over the effect

of individual parameters. The study further shows that over the ECS the effect of RH and LTS on the CER/AOD relationship is opposite to that of pressure vertical velocity (PVV). Over the YRD, The CER is larger in unstable atmospheric conditions than in stable conditions, irrespective of the AOD and the CER is much larger in high relative humidity conditions than in low relative humidity conditions.

**Key words:** AOD, Cloud parameters, LWP, Geographical detector method, Confounding effects, MODIS, East China

## 1 Introduction

The atmosphere is primarily composed of gases, i.e. nitrogen, oxygen and several noble gases, as well as a wide variety of trace gases that occur in relatively small and highly variable amounts. In addition, liquid and solid particles are suspended in the atmosphere. The suspension of solid and liquid particles in the gaseous medium is technically defined as an aerosol, but in practice usually the term aerosol refers to the particulate component only (Seinfeld and Pandis, 1998). The aerosol particles originate from a large variation of both direct and indirect sources, and the concentrations and chemical and physical properties of aerosol particles change under the influence of a variety of atmospheric processes and which thus are variable in space and time. The residence time of tropospheric aerosol particles varies from hours to weeks (Bellouin et al., 2020), depending on particle size and atmospheric conditions. Directly emitted aerosol types include, e.g., sea spray, dust, smoke, volcanic ash, pollen etc. The indirect/Secondary formation of aerosol particles occurs through nucleation and subsequent growth by physical and chemical processes such as condensation, coagulation and multiphase chemical reactions on the particle surface, involving precursor gases such as sulphur dioxide (SO<sub>2</sub>), nitrogen dioxide (NO<sub>2</sub>), ammonia (NH<sub>3</sub>), volatile organic compounds (VOCs), etc.

Aerosol particles are important for climate, air quality and heterogenous chemical processes. Aerosol particles exert a direct effect on climate by their interaction with radiation (aerosol radiation interaction, ari) which exerts a radiative forcing (RF<sub>ari</sub>) on the Earth's energy budget which results in rapid adjustments of global mean atmospheric quantities such as temperature. The sign and strength of radiative forcing (RF) due to ari  $-(RF_{ari})$  vary with environmental parameters (Bellouin et al., 2020). In particular, aerosol particles by scattering incoming solar radiation back into space, but the effect of RF<sub>ari</sub> depends on the brightness of the aerosol with respect to that of the underlying surface. The scattering of (bright) aerosol

90 ~~over a darker surface which~~ results in cooling and reduction of the warming effect of greenhouse gases (GHG). ~~while~~ In contrast, the interaction of absorbing aerosol particles with solar radiation may result in local heating and thus reinforce the GHG effect and influence meteorological processes.–

Aerosol particles can act as cloud condensation nuclei (CCN, in liquid clouds) or ice nucleating particles (INP, in ice clouds), depending on their chemical composition and size. ~~When CCN, when they~~ are activated they can ~~exert an indirect effect on climate by modify changing the~~ cloud microphysical properties and precipitation and thus indirectly influence the Earth's radiative budget (aerosol-cloud interactions, aci) (Tao et al., 2012; Fan et al., 2016; Rosenfeld et al., 2019; Rao and Dey, 2020; Bellouin et al., 2020). An increase in CCN concentrations leads to an increase in the number of cloud droplets ( $N_d$ ) and, if ~~The first indirect effect of aerosols, often referred to as the "Twomey" effect (Twomey, 1977; Matheson et al., 2005; Koren et al., 2005; Meskhidze and Nenes, 2010; Costantino et al., 2010; 2013), describes the effect of the increase of the number of aerosol particles when~~ the cloud liquid water path (LWP) remains unchanged, ~~which results in the increase in the number of cloud droplets and~~ the decrease of the cloud droplet effective radius (CER). The smaller CER in turn results in the enhanced reflection of solar radiation and thus cloud albedo and enhanced RF due to aci ( $RF_{aci}$ ). This effect of the increase of the number of aerosol particles on cloud properties at constant LWP is often referred to as the "Twomey" effect (Twomey, 1977; Feingold, et al., 2001; Matheson et al., 2005; Koren et al., 2005; Meskhidze and Nenes, 2010; Costantino et al., 2010; 2013 ~~(Twomey, 1977; Feingold, et al., 2001)~~. Another component of  $RF_{aci}$  are rapid adjustments which may also lead to the modification of other cloud properties in response to the increase of  $N_d$  and decrease in CER, such as a ~~The second indirect effect describes the~~ decrease in precipitation efficiency ~~due to the decrease in the size of the cloud droplets~~, resulting in the increase of the LWP and the amount of clouds, thus enhancing the reflection of solar radiation (Albrecht, 1989). ~~These two~~ –first and second indirect effects of aci are also referred to as the cloud albedo and cloud lifetime effects (Quaas et al., 2008).

The CER is an important factor affecting cloud physical processes and optical properties, ~~which in turn influence precipitation and the Earth's radiation balance~~. Slingo (1990) pointed out that a reduction in the average CER by 15% - 20% can balance the radiative forcing at the top of the atmosphere caused by a doubling of carbon dioxide. Therefore, small changes in cloud microphysical properties may lead to important climate impacts (Zhao et al., 2018). Further study on the sensitivity of CER to relations

120 ~~between aerosols ( $S_{CER,A}$ , further referred to as  $S$ ) and CER~~, together with meteorological parameters  
influencing ~~aerosol-cloud interaction~~aci, can improve our understanding of these processes ~~and the~~  
~~effects of aci on RF~~, leading to improved aerosol-cloud parameterizations in regional climate models.  
The variation in  $N_d$  with CCN is referred to as the susceptibility  $\beta$  ( $\beta = d \ln N_d / d \ln A$ ; e.g., Gryspeerdt  
et al. (2023)) and the variation of CER with CCN is referred to as the sensitivity  $S$  (eq. 1 in Section 3.1).  
125 ~~Much of the variation of aerosol-cloud effective radiative forcing in ensembles of climate models is due~~  
~~to the variation in  $\beta$ , while  $\beta$  is also central to the strength of cloud adjustments (Gryspeerdt et al., 2023).~~  
The ~~sensitivity of effects of aerosols on the~~ microphysical ~~characteristics-properties~~ of clouds ~~to aerosol~~  
have been studied based on data from a large number of monitoring campaigns, using satellite, aircraft  
and ground based observations, and by using model simulations. Because of the large spatial coverage  
~~and high spatial and temporal resolution~~, satellite instruments have been widely used to study aerosol-  
130 cloud interaction in different conditions, confirming the ~~large influence~~high sensitivity of of aerosol  
~~particles on~~ cloud properties ~~to aerosol~~ (e.g., Yuan et al., 2008; Rosenfeld et al., 2014; Saponaro et al.,  
2017; Liu et al., 2018; Pandey et al., 2020; Christensen et al., 2020; Liu et al., 2021). ~~In In~~ studies ~~on S~~  
~~of the first indirect effect of aerosols with~~utilizing satellite data, ~~which is the subject of the current study,~~  
the aerosol optical depth (AOD) is ~~often~~ used as a proxy for the aerosol concentration, ~~which is justified~~  
135 ~~by the correlation of AOD and CCN published by Andreae (2009). However, AOD is determined by all~~  
~~aerosol particles in the atmospheric column, including particles that do not act as CCN, depends on the~~  
~~relative humidity (RH) throughout the atmospheric column, does not provide information on chemical~~  
~~composition and may be influenced by aerosol in disconnected layers. The use of the Aerosol Index (AI),~~  
~~the product of AOD and the Ångström Exponent (AE; describing the spectral variation of AOD), is~~  
140 ~~suggested as a better indicator of CCN because AE includes information on aerosol size (e.g., Nakajima~~  
~~et al., 2001). However, the AE is determined from AOD retrieved at two or more wavelengths and the~~  
~~evaluation of the results versus ground-based reference data shows the large uncertainty in AE. Therefore,~~  
~~in recent MODIS product Collections, AE is not provided over land (e.g., Levy et al., 2013; Kourtidis et~~  
~~al., 2015). AE is also not well-defined for low AOD for which uncertainty is largest (Bellouin et al., 2020;~~  
145 ~~Gryspeerdt et al., 2023). The issues associated with using AOD or AI as proxy for CCN were discussed~~  
~~by, among others, Rosenfeld et al. (2014) who~~ ~~do not recommend the use of AI while also concluding~~  
~~that no better proxy is available. Therefore, in this study, AOD is used as a proxy for CCN to study S. It~~

is noted that in other studies, e.g., Jia et al., 2022, both AOD and AI have been used and the results show similar behaviour.

150 Many of these studies confirmed the Twomey effect (e.g., Chen et al., 2014; Christensen et al., 2016; Jia et al., 2019). However, other studies show that, over some areas and especially over land in situations with high AOD, the CER increases with the increase of AOD, in contrast to the hypothesis of the “Twomey effect” (e.g., Feingold et al., 2001; Yuan et al., 2008; Grandey and Stier, 2010; Tang et al., 2014; Wang et al., 2015; Jia et al., 2019; Liu et al., 2020). It is noted that in these studies, the relationship  
155 between CER and aerosol concentration was not constrained by LWP, although this is the premise of the Twomey effect first indirect effect of aerosol.

Meteorological conditions are important factors determining both the occurrence of clouds and cloud properties and therefore, in aerosol-cloud interaction (ACI) studies, the variation of meteorological conditions needs to be considered together with the variation of AOD (e.g., Myhre et al., 2007; Tang et al., 2014). On the one hand, the meteorological parameters have the impacts on influence the Twomey effect. Jones et al. (2009) concluded that vertical motion, aerosol type, and aerosol layer heights do make a significant contribution to  $RF_{aci}$  first aerosol indirect effect (AIE) and that these factors are often more important than total aerosol concentration alone and that the relative importance of each differs significantly from region to region. Su et al. (2010) studied demonstrated the influence of pressure vertical velocity (PVV) ( $\omega_{700hPa}$ ) on the S first indirect effect of aerosols and demonstrated the effect of this parameter on the CER and the LWP. Wang et al. (2014) proved that the well-recognized aerosol effect mingled with meteorological conditions (RH and PVV), which likely is the main reason for the positive values of  $S\beta_{ln CER - ln AOD}$  (the change of CER with the change of AOD, see Section 3.1) over land. Tang et al. (2014) observed the Twomey effect over ocean, but a positive CER-AOD relationship over  
160  
165  
170 Eastern China which they attributed to changes in relative humidity and wind fields. Tang et al. (2014) concluded that “Our results suggest that the effect of meteorology may not be negligible when investigating the aerosol indirect effect on a large scale, especially when the weather conditions are complex and change frequently.” Andersen and Cermak (2015) studied biomass burning aerosol over the Atlantic Ocean (Sep-Dec) in stable and unstable environments (LTS) and observed that the aerosol  
175 effect is stronger in unstable environment, especially during biomass burning episodes. These authors concluded that “the observed absolute differences in CER between stable and unstable environments are

driven by cloud dynamical effects (CER and LWP are positively associated), or meteorology”, Jia et al. (2020) inferred that  $S$  increases remarkably with both cloud-base height and cloud geometric thickness (proxies for vertical velocity at cloud base), suggesting that stronger aerosol-cloud interactions generally occurs under larger updraft velocity conditions. On the other hand, the meteorological parameters also have the impacts on influence the potential adjustments. Koren et al. (2010) reported that observed cloud top height and cloud fraction correlate best with model pressure updraft velocity and relative humidity. Quaas et al. (2010) discussed the relationship between total cloud cover and AOD, often observed in satellite data, based on model simulations to test six hypotheses. These authors concluded that the increase of aerosol optical depth that accompanies the swelling of aerosol particles in humid airmasses is the dominant process contributing to the observed correlation, confirming earlier conclusions by Myhre et al. (2007). Boucher and Quaas (2012) reported that aerosol humidification has a large impact on the relationship between AOD and rain rate and that discriminating the data into classes of pressure vertical velocity and/or relative humidity does not eliminate these meteorological effects.

Gryspeerd et al. (2014) studied the relationship between aerosol and initial cloud cover as a function of relative humidity  $RH$  ( $RH_{850hPa}$ ) and vertical convection strength ( $\omega_{500hPa}$ ). Wang et al. (2014) proved that the well-recognized aerosol effect mingled with meteorological conditions ( $RH_{750hPa}$  and  $\omega_{750hPa}$ ), which likely is the main reason for the positive aerosol-cloud interaction (ACI) index (defined in Section 3.1) values of  $\beta_{\ln CER - \ln AOD}$  (the change of CER with the change of AOD, see Section 3.1) over land.

Wang et al. (2015) discussed  $S_{CER-A}$  the increase of CER with AOD in high AOD conditions over eastern China, which was observed during the summer but not in the winter, in terms of meteorological conditions. In particular they considered the different humidity effects during these seasons. Liu et al. (2017) showed that the formation of large cloud droplets in both horizontal and vertical directions and the increase in cloud cover are is promoted in an environment with high relative humidity  $RH$  ( $RH_{950hPa}$ ).

A rising air mass ( $\omega_{750hPa}$ ) can promote the formation of thicker and higher clouds. Tang et al. (2014) observed the Twomey effect over ocean, but a positive CER-AOD relationship over Eastern China which they attributed to changes in relative humidity and wind fields. Tang et al. conclude that “Our results suggest that the effect of meteorology may not be negligible when investigating the aerosol indirect effect on a large scale, especially when the weather conditions are complex and change frequently.” Quaas et al. (2010), discuss the relationship between total cloud cover and AOD, often observed in satellite data,

based on model simulations to test six hypotheses. These authors conclude that the increase of aerosol optical depth that accompanies the swelling of aerosol particles in humid airmasses is the dominant process contribution to the observed correlation, confirming earlier conclusions by Myhre et al (2007). Boucher and Quaas (2012) report that aerosol humidification has a large impact on the relationship between AOD and rain rate and that discriminating the data into classes of pressure vertical velocity and/or relative humidity does not eliminate these meteorological effects. Anderson and Cermak (2015) studied biomass burning aerosol over the Atlantic (Sep-Dec) in stable and unstable environments (LTS) and observed that the aerosol effect is stronger in unstable environment, especially during biomass burning episodes. These authors concluded that “the observed absolute differences in CER between stable and unstable environments are driven by cloud dynamical effects (CER and LWP are positively associated, or meteorology)”

The above are examples of ~~Only few~~ studies ~~have~~ addressed ~~ing~~ the influence of different aerosol and meteorological parameters on the ~~sensitivity of cloud parameters to aerosol and potential confounding effects~~. ~~Indirect effect and~~ most of them used traditional statistical methods ~~or stratified the data according to confounding meteorological parameters (-e.g., Saponaro et al., 2017; Ma et al., 2018)~~. In the current study the geographical detector method (GDM) is applied ~~as a complementary tool~~ to quantify the relative importance of the effects of nine parameters on ACIS. The GDM ~~is explained in detail in Section 3.2. In brief, is~~ a set of statistical methods ~~is used~~ to detect the spatial variability of aerosol and cloud properties, which are spatially differentiated, and evaluate the occurrence of correlations in their behaviour and the driving forces behind these correlations (Wang and Hu, 2012; Wang et al., 2016). The basic idea of the GDM is that the spatial distributions of two variables tend to be similar if these two variables are connected (Zhang and Zhao, 2018). The method ~~can be~~ used ~~in this study~~ to analyse the relative importance of ~~different influencing factors, and interactions between them, influencing on ACIaci~~.

The focus of the current study is to establish a CER-aerosol parameterization scheme by the application of the GDM to satellite data over two contrasting areas, i.e. the Yangtze River Delta (YRD) in eastern China, with high aerosol concentrations, and a relatively clean area over the East China Sea (ECS). The satellite data are first used to ~~study the build a relationship between~~ CER ~~sensitivity to and the~~ aerosol ~~concentration (using AOD as a proxy)~~ for different AOD regimes and all LWP values, followed by



235 constraining the LWP in different intervals. It is noted that  $RF_{aci}$  is formulated in terms of  $N_d$ —the cloud droplet number concentrations  $N_d$ , whereas studies on the Twomey effects often use CER instead of  $N_d$ . CER is readily available as a satellite retrieval product, although in particular over land the reliability is questioned (Grandey and Stier, 2010), whereas  $N_d$  is derived from CER and the cloud optical thickness (COT) (e.g., Grandey and Stier, 2010; Arola et al., 2022). This implies that  $N_d$  is subject to the same  
240 retrieval errors as CER, including a possible relation between CER and LWP. The comparison of global maps of the sensitivities of CER and  $N_d$  to AOD by Grandey and Stier (2010) exhibits very similar patterns. In this study, the CER sensitivity to AOD is stratified by LWP, which however poses problems in the evaluation of  $RF_{aci}$ . However, the current study focuses on understanding effects of different parameters on CER sensitivity to aerosol rather than the application to determine  $RF_{aci}$ .  
245 The results from the CER sensitivity study are used to guide Next the application of GDM is applied to determine the relative effects of different parameters on ~~the  $ACI_{aci}$~~ . Relations between CER and AOD, meteorological conditions and several cloud properties are ~~analysis~~ determined, including combined effects of different influencing parameters.

## 2 Approach

### 250 2.1 Study area

The complex aerosol composition and the high aerosol concentrations render eastern China an interesting area for a variety of studies of processes involving aerosols, including the current study on the use of satellite data for the systematic assessment of aerosol indirect effects $_{aci}$ , i.e., S, adjustments and confounding meteorological factors-. The ~~ACI~~ study focuses on two areas, i.e. the Yangtze River Delta  
255 (YRD, 2726°N-35°N; 114113°E-122°E) in eastern China and the East China Sea (ECS, 2019°N-28°N; 126125°E-134°E). The locations of the YRD and the ECS are shown in the map in Figure 1.

The YRD has a developed economy, with much industrial activity, large harbors (sea and river) and related busy ship traffic, dense populations in large urban centers, all with high traffic intensity and high energy consumption. In addition to the direct emission of black carbon, also aerosol precursor gases such  
260 as  $NO_2$ ,  $SO_2$  and VOCs are emitted from the combustion of biomass, coal and petrochemical fuels, leading to the formation of secondary aerosol particles such as nitrate and sulfate aerosols, while agricultural activities result in the emission of dust, ammonia and biological VOCs (BVOCs) into the

atmosphere. These activities and associated emissions result in the occurrence of high AOD over the YRD. Over the East China Sea (ECS) the main aerosol types are sea spray aerosol generated by the interaction between wind and waves and anthropogenic pollutants transported from the [land-Asian continent over the ocean](#) in the East Asian outflow. During transport over hundreds of km, aerosol particles are removed by several processes such as dry and wet deposition and hence the aerosol concentrations decrease and the AOD becomes relatively low and is dominated by sea spray aerosol. In view of the differences in aerosol composition and concentrations, the polluted YRD area and the relatively clean ECS area were selected as contrasting regions for the study of the influence of aerosols on cloud properties over land and over ocean.

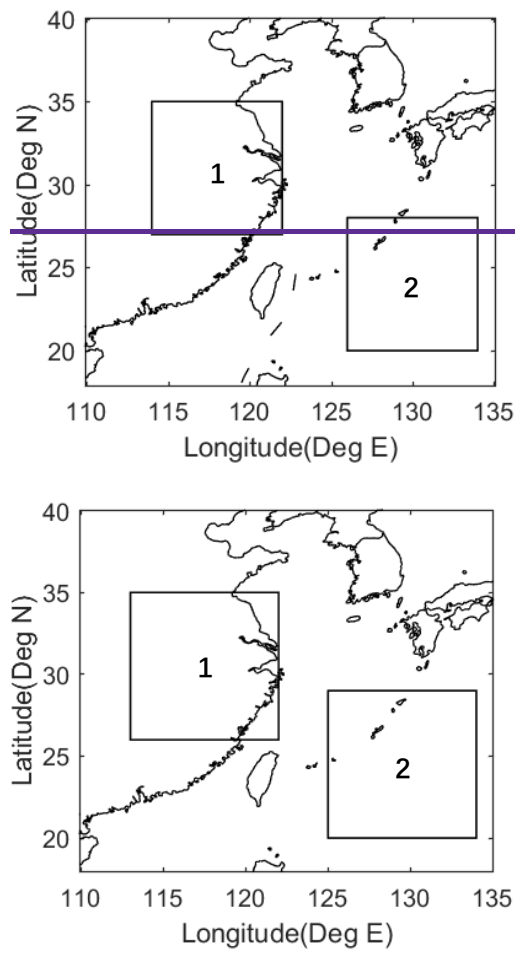


**Figure 1. Map showing the locations of the two study areas selected for aerosol - cloud interaction studies: area 1 is the Yangtze River Delta (YRD;  $2726^{\circ}\text{N}$ - $35^{\circ}\text{N}$ ,  $114113^{\circ}\text{E}$ - $122^{\circ}\text{E}$ ), and area 2 indicates the selected Eastern China Sea [area](#) (ECS; [area](#) ( $2019^{\circ}\text{N}$ - $28^{\circ}\text{N}$ ,  $126125^{\circ}\text{E}$ - $134^{\circ}\text{E}$ ).**

## 2.2 Data used

In this study, aerosol and cloud properties were used which were derived from measurements from the Moderate Resolution Imaging Spectroradiometer (MODIS) on-board the Aqua satellite, for the period 2008-2022 (15 years). This data was selected because the MODIS data are widely used and therefore they are well-characterized. In addition, the Aqua satellite flies in an afternoon orbit with local overpass time around 13:30, when the atmospheric boundary layer is well-developed. MODIS L3 Collection 6.1 daily aerosol and cloud parameters were downloaded from the LAADS website ([Liu, 2022](https://ladsweb.modaps.eosdis.nasa.gov/)~~https://ladsweb.modaps.eosdis.nasa.gov/~~, last access: 12 July 2022) with a spatial resolution of  $1^\circ \times 1^\circ$ . ~~Aerosol retrieval is only executed in clear sky conditions whereas cloud properties can only be retrieved in cloudy skies. Hence, it is not possible to obtain co-located aerosol and cloud data from satellite. For satellite-based aci studies it is assumed that, following, e.g., Jia et al. (2022), aerosol properties are homogeneous enough to be representative for those in adjacent cloud areas. Consequences of this assumption were discussed by McComiskey and Feingold (2012). The utilization of the daily MODIS aerosol and cloud data at  $1^\circ \times 1^\circ$  resolution ensures that they are coincident when investigating aerosol-cloud interaction.~~ The MODIS instrument has 36 spectral bands - aerosol properties are retrieved using the first seven of these (0.47-2.13  $\mu\text{m}$ ) (Remer et al., 2005; Levy et al., 2013; Sayer et al., 2014; [2017](#)) while additional wavelengths in other parts of the spectrum are used for the retrieval of cloud properties (Platnick et al., 2003; [2017](#)). ~~More d~~Detailed information on algorithms for the retrieval of aerosol and cloud properties is provided at ~~\_~~<http://modis-atmos.gsfc.nasa.gov> (last access: 01 July 2021). In this study we use the AOD at 550 nm (referred to as AOD throughout this manuscript), CER, ~~cloud optical thickness~~ (COT), cloud liquid water path (LWP), cloud top pressure (CTP), cloud fraction (CF) and cloud top temperature (CTT). ~~The MODIS Collection 6.1 AOD product over China has been validated by, e.g., Che et al. (2019) and globally over land and ocean by Wei et al. (2019). MODIS C6.1 cloud products were evaluated by Platnick et al. (2017). The validation of CER and LWP, the primary cloud products used in this paper, was described by Painemal and Zuidema (2011), who compared MODIS C5 with in situ data (aircraft), and likewise the MODIS C6.1 CER product was evaluated by Fu et al. (2022) by comparison with airborne measurements. Fu et al. (2022) concluded that their “validation, along with in situ validation of MODIS CER from other regions (e.g., Painemal and Zuidema, 2011; Ahn et al., 2018), provides additional confidence in the global distribution of bias-adjusted MODIS CER~~

reported in Fu et al. (2019).” It is noted that COT and CER are retrieved whereas LWP is secondarily derived (e.g., Painemal and Zuidema, 2011). AOD is used as a proxy for the amount of aerosol particles CCN in the atmospheric column to investigate ACI<sub>aci</sub> (Andreae, 2009; Kourtidis et al., 2015) which seems to be the best alternative (Rosenfeld et al., 2014). As discussed in the Introduction, the use of an AE-based correction is not recommended over land (e.g., Kourtidis, et al., 2015). Comparisons with surface-based sun photometer data revealed shows that Collection 6 should improves upon Collection 5, and overall, 69.4% of MODIS Collection 6 AOD fell within the expected uncertainty of  $\pm (0.05 + 15\%)$  (Levy et al., 2013; Tan et al., 2017). To reduce a possible overestimation of the AOD (e.g., due to cloud contamination), cases with AOD greater than 1.5 were excluded from further analysis. The choice of this threshold, rather than 0.6 used by Brendan et al. (2006), who used MOD06 Collection 04 products, is based on reports by Christenson et al. (2017) and (Varnáí and Marshak, 2009). Christenson et al. (2017) used MOD06 C6 data (1km x1km) and reported that “large aerosol optical depths remain in the MODIS-observed pixels near cloud edges, due primarily to 3-D effects (Varnáí and Marshak, 2009) and the swelling of aerosols by higher relative humidity.” Varnáí and Marshak (2009) noted that beyond 15 km contamination effects were minimized in MODIS data (1km x1km). Furthermore, we discarded scenes (1° by 1°) in which the aerosol distribution is heterogeneous, i.e. with a standard deviation higher than the mean value (Saponaro et al., 2017; Jia et al., 2022). As most aerosol particles are located in the lower troposphere (Michibata et al., 2014), the focus in this study is on warm clouds with CTT larger than 273K, CTP larger than 700 hPa and LWP smaller than 200 g m<sup>-2</sup>. LWP larger than 200 g m<sup>-2</sup> is excluded to avoid deep convective clouds (Wang et al., 2014). Transparent-cloudy pixels (COT<5) were discarded to limit uncertainties (Grosvenor et al., 2018). The solar zenith angle was restricted to SZA < 65° and the viewing zenith angle to VZA <55° to avoid the large biases in COT and CER retrievals at larger angles (Grosvenor et al., 2018). Cloud parameters were only considered in single liquid layer clouds. To ensure that the data used only included consisted of single layer liquid layer clouds and, as well as nonprecipitating cases, we applied the same filtering criteria as described by Saponaro et al. (2017) were applied to the MODIS cloud data. ~~Cloud works on precipitation filtering-reprocess~~

~~Confounding Effects of~~ meteorological conditions effects on ACI<sub>aci</sub> were explored using the daily temperature at the 700 and 1000 hPa levels, relative humidity (RH) at the 750 hPa level and pressure vertical velocity (PVV) at the 750 hPa level. Low tropospheric stability (LTS), which is defined as the

335 difference in potential temperature between the free troposphere (700 hPa) and the surface (1000 hPa),  
 is used as a measure of the strength of the inversion that caps the planetary boundary layer (Klein and  
 Hartmann, 1993; Wood and Bretherton, 2006). These meteorological data were retrieved from the  
 ECMWF ERA-5 reanalysis data which provide global meteorological conditions at 0.25°x0.25°  
 resolution for 37 pressure levels in the vertical (1000-1 hPa), for every 1 h (UTC) ([Liu,  
 2022](https://cds.climate.copernicus.eu/cdsapp#!/dataset/reanalysis-era5-pressure-levels-monthly-means?tab=form)~~https://cds.climate.copernicus.eu/cdsapp#!/dataset/reanalysis-era5-pressure-levels-monthly-  
 means?tab=form, last access: 12 July 2022~~). The meteorological parameters were resampled to the  
 MODIS/Aqua overpass time at 13:30 (local time) by taking a weighted average ~~of the properties~~ at the  
 two closest times (05:00 UTC and 06:00 UTC) provided by [the ECMWF ERA-5 reanalysis data](https://cds.climate.copernicus.eu/cdsapp#!/dataset/era5-interim)~~ERA  
 Interim~~.

345 **Table 1. The list of the parameters used, sources, and their corresponding temporal-spatial resolutions  
 applied in the present study, together with the sources, time periods and spatial resolutions.**

<u>Source</u>	<u>Time period</u>	<u>Resolution</u>	<u>Parameters</u>
<u>MYD08</u>	<u>Jan 2008-Dec 2022</u>	<u>Daily, 1°x1°</u>	<u>AOD at 550 nm</u> <u>COT at 2.1 um</u> <u>CER at 3.7 um and 2.1 um</u> <u>Cloud-top temperature</u> <u>Cloud-top pressure</u> <u>LWP at 2.1 um</u> <u>Cloud Fraction</u> <u>Solar zenith angle</u> <u>Sensor zenith angle</u> <u>Cloud multi-layer flag</u> <u>Cloud phase flag</u>
<u>ERA5</u>	<u>Jan 2008-Dec 2022</u>	<u>hourly, 0.25°x0.25°</u>	<u>Temperatures at 700 and 1000 hPa</u> <u>Relative humidity at 750 hPa</u> <u>Vertical velocity at 750 hPa</u>

### 3 Methods

#### 3.1 Sensitivity of Aerosol-cloud interaction index parameters to changes in aerosol concentrations

350 ~~The first indirect effect of aerosols is defined as the variation of~~ Changes in aerosol loading lead to an  
 adjustment of cloud optical or microphysical parameters (~~cloud optical thickness, cloud droplet effective~~

radiusCOT, CER, etc.) ~~with the variation of aerosol loading~~. Aerosol particles can become ~~cloud condensation nuclei (CCN) or ice nucleating particles (INP)~~, depending on their chemical composition ~~and ambient temperature~~. When these nuclei are activated, they become cloud droplets due to condensation of water vapor. When the concentration of aerosol particles increases, often also the number of CCN or INP ~~may increase~~ and thus the number of cloud droplets ~~may increase~~. However, if the liquid water content in the cloud does not change (as indicated by a constant LWP), the condensable water will be distributed over more cloud droplets which thus remain smaller, i.e. the CER decreases and the cloud albedo increases when the aerosol concentration increases. On the basis of findings of Kaufman and Fraser (1997), Feingold et al. (2001) pointed out that the ~~sensitivity of cloud microphysical properties (e.g. CER) to changes in aerosol (e.g., AOD) can be described by aerosol-cloud interaction caused by the first indirect effect can be calculated by~~ the following formula:—

$$S = S_{\text{CER-AOD}} = \text{ACI}_r = - \left. \frac{d \ln r_e}{d \ln \alpha} \right|_{\text{LWP}} \quad 0 < \text{SACI}_r < -0.33 \quad (1)$$

Where  $r_e$  represents the ~~cloud droplet effective radius (CER)~~ and  $\alpha$  represents the ~~aerosol number concentration AOD~~. Following Andreae (2009), AOD and CCN are correlated and AOD varies with CCN following a power law relationship. Equation Eq. (1) describes the ~~relative~~ change of CER with the ~~relative~~ change of the ~~aerosol concentration AOD~~ for constant LWP. ~~It is noted that this formulation differs from that used in recent studies (e.g., Bellouin et al., 2020) where S is expressed in the cloud droplet number concentration  $N_d$  with no restriction in LWP. The sensitivity~~ ~~In this study, the AOD is used as a proxy for the aerosol number concentration and~~ ~~ACI<sub>r</sub> S of CER to AOD~~ can be determined as the slope of a linear fit to a log-log plot of CER versus AOD. It is noted that ~~SACI<sub>r</sub>~~ is a function of CER and effects on CER directly influence ~~SACI<sub>r</sub>~~. In this study effects on ~~ACI<sub>r</sub>~~ (from here on simply denoted as ~~SACI~~) and CER are used ~~interchangeably~~ ~~intermittently~~. ~~Relations between CER and AOD are determined through Eq. 1 and correlation coefficients R. The significance of these correlations was determined by using the student's t test, i.e. the results are statistically significant when the p value is smaller than 0.01, where p is defined as the probability of obtaining a result equal to or "more extreme" than what was actually observed.~~

### 3.2 Geographical detector method

The geographical detector method (GDM) is introduced to analyze which factors influence the ~~ACI<sub>r</sub>~~

380 [and identify possible correlations between different factors](#). The GDM is based on the assumption that if an independent variable has an important influence on its dependent counterpart, their spatial distributions should also have evident similarities (Wang and Hu, 2012; Wang et al., 2016). ~~4~~[The GDM not only takes accounts of for the rank order of the variables as determined by the Spearman's Rank method but also spatial information](#). The geographical detector provides four modules, including ~~the~~ factor detector, interaction detector, risk detector and ecological detector. In this study, the first two modules are used to detect interactions between different parameters, based on their spatial variations, and thus reveal the driving factors for aerosol-cloud interaction over the target regions. The influencing factors ( $x$ ) considered in this study are aerosol and meteorological parameters and the dependent factors ( $y$ ) are [the ACL index](#) and cloud parameters. In the GDM, for example, the CER data are recorded in a raster grid as illustrated in Figure 2. The data in the raster grid is transformed into dot files, each dot containing a value for the CER and for one of the influencing parameters  $x$ . The dependent (CER) and influencing ( $x$ ) parameters are separated into 2 layers with the same grid. In the  ~~$x$~~  layer, the Jenks natural breaks classification method (Brewer and Pickle, 2002), aiming to minimize the variance within the group and maximize the variance between groups, was applied to categorize the whole region into  ~~$N_i$~~  sub-regions (3 in Figure 2), according to pre-defined ranges of influencing factors (e.g., AOD). In each [sub-region spatial unit \( \$N\_i\$ \)](#), the influencing factor ( $x$ ) varies within certain limits, with variance  $\sigma_i$ . The power of determination  $q$  of  ~~$x$~~  to  ~~$y$~~  (also referred to as power of the influencing factor) determines the extent to which a factor ( $x$ ) influences the dependent factor ( $y$ ) over the whole study area and is calculated using [Equation-Eq. \(2\)](#):

395

$$400 \quad q = 1 - \frac{\sum_i^L N_i \sigma_i^2}{N \sigma^2} \quad (2)$$

where  $i$  (1, ..., L) is the number of sub-regions of factor  ~~$x$~~ ;  $N$  represents the total number of spatial units over the entire study area;  $N_i$  denotes the number of samples in sub-region  $i$ ; and  $\sigma_i^2$  and  $\sigma^2$  denote [the s](#)-variance of [the](#) samples in the subregion  $i$  and the total variance in the entire study area, respectively. The value of  ~~$q$~~  varies between 0 and 1, i.e.  $q \in [0,1]$ , where 0 indicates that factor  ~~$x$~~  has no influence on  $y$  and the closer  $q$  is to 1, the greater the influence of  ~~$x$~~ . For instance, if  $q = 0.5$ ,  ~~$x$~~  can explain 50% of the variation of  ~~$y$~~ . In this study, multi-years [of](#) mean values of influencing factors ( $x$ ) and dependent factors ( $y$ ) [were](#) calculated for each raster grid. Then, we classified the influencing factors (e.g. AOD and meteorological parameters) into 5 sub-regions by the Jenks natural breaks classification

405

method (Brewer and Pickle, 2002). For example, AOD needs to be classified into 5 levels using the Jenks natural breaks classification method, and the AOD source data needs to be reclassified into 1-5 natural numbers from small to large, and then counted into the grid. Therefore, the input of the independent variable AOD is a type variable. However, it should be noted that the GDM also has unstable characteristics. On the one hand, it is due to the MAUP (Modified Area Unit Problem) variable area unit problem, which can be understood as the influence of "scale effect". Due to the limitation of data resolution used in this study, the spatial statistical unit is  $1^{\circ} \times 1^{\circ}$ . On the other hand, the methods used for data discretization can also have an impact. This study attempts to determine the optimal number of classifications by examining the impact of number of classification levels (3-8) on the GDM output results. The results show that the number of classification levels does not affect the relative importance of cloud factors on the cloud. Here we classify the values of each cloud factor into 5 levels during the period of 2008-2022.

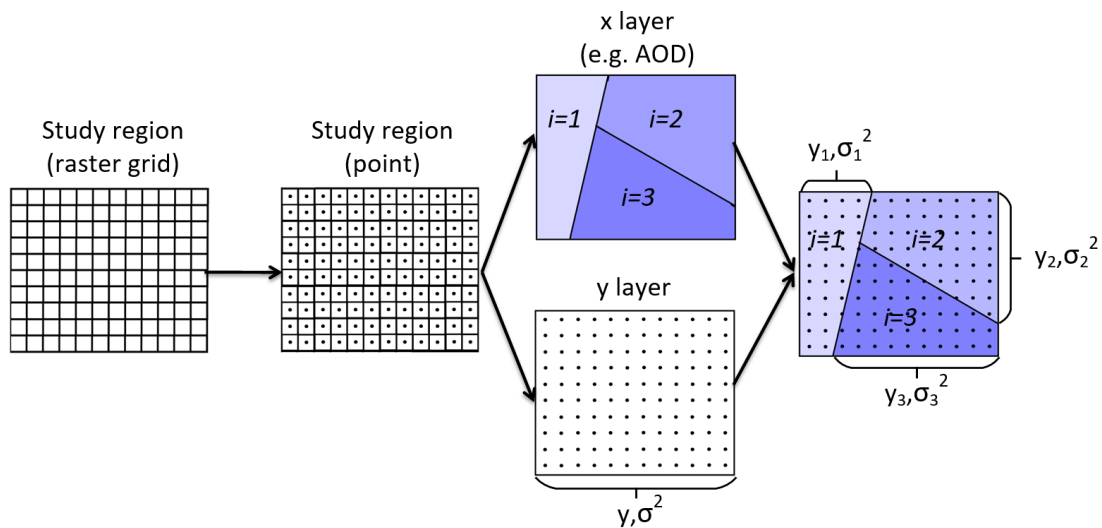


**Figure 2. The principle of the geographical detector method. See text for explanation.**

The interaction detector can be used to test for the influence of interaction of between different influencing factors and to determine whether the interaction of two factors, e.g.,  $x_1$  and  $x_2$ , on the dependent factor ( $y$ ) and whether this interaction weakens or enhances the influence of each of  $x_1$  or  $x_2$  on the dependent variable,  $y$ , or whether they are independent in influencing  $y$ . For example, Figure 3(a) showed the spatial distribution of the dependent variable,  $y$ . The factors  $x_1$  and  $x_2$  both vary across the study region, but in different ways, and for each factor different sub-regions can be distinguished by application of the Jenks classification method described above to each factor separately. This is as illustrated in Figures 3(b) and 3(c) where, as an example, for each factor three different sub-regions are



considered for each factor), as shown in Figure 3(b) and 3(c). Usually, the dependent variable  $y$  is influenced by several different factors  $x_i$ , (Figure 3) and the combined effect of two or more factors may have a weaker or stronger influence on  $y$  than each of the individual factors. The  $q$  values for the influences of factors  $x_1$  and  $x_2$  on  $y$ , obtained from the application of the factor detector method (equation Eq. 2), may be represented as  $q(x_1)$  and  $q(x_2)$ . Hence, a new spatial unit and subregions may be generated by overlaying the factor strata  $x_1$  and  $x_2$ , written as  $x_1 \cap x_2$ , where  $\cap$  denotes the interaction between factor strata  $x_1$  and  $x_2$  as illustrated in Figure 3(d). Thus, the  $q$  value of the interaction of  $x_1 \cap x_2$  may be obtained, represented as  $q(x_1 \cap x_2)$ . Comparing the  $q$  value of the interaction of the pair of factors and the  $q$  value of each of the two individual factors, five categories of the interaction factor relationship are described can be considered which are as summarized in Table 4.2. If  $q(x_1 \cap x_2) > q(x_1) + q(x_2)$ , this is referred to as a nonlinear enhancement of two variables. And if  $q(x_1 \cap x_2) > \text{Max}[q(x_1), q(x_2)]$ , this is referred to as a bilinear enhancement of two variables. The occurrence of nonlinear enhancement and bilinear enhancement is are indicated with the  $q$  values in Table 2 and in the caption of Figure 7 in the revised manuscript.

It is noted that the  $q$  values of multiple influencing factors are considered separately they may sum up to larger than 100%. However, when the variables are correlated they must be considered together and the interaction  $q$  value must be evaluated.

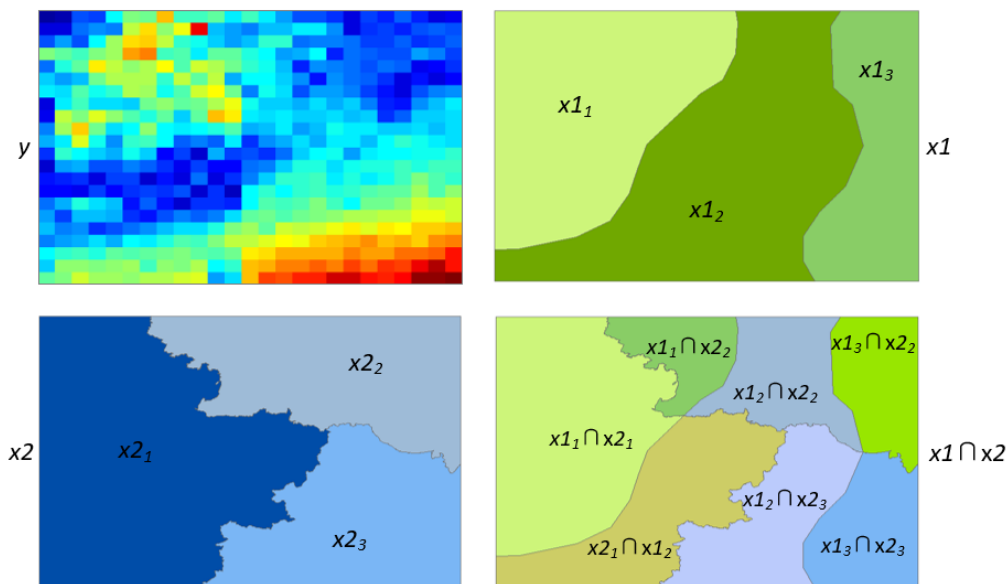







Figure 3. Detection of interaction (see text for explanation).

**Table 12. Interaction categories of two factors and the interaction relationship**

<u>Illustration</u>	<u>Description</u>	<u>Interaction</u>
	$q(x1 \cap x2) < \text{Min}[q(x1), q(x2)]$	Weakened, nonlinear
	$\text{Min}[q(x1), q(x2)] < q(x1 \cap x2) < \text{Max}[q(x1), q(x2)]$	Weakened, unique
	$q(x1 \cap x2) > \text{Max}[q(x1), q(x2)]$	Enhanced, bilinear
	$q(x1 \cap x2) = q(x1) + q(x2)$	Independent
	$q(x1 \cap x2) > q(x1) + q(x2)$	Enhanced, nonlinear

455 The geographical detector method has been used to detect influencing factors for several different purposes (e.g., Wang et al., 2018; Zhang and Zhao, 2018; Zhou et al., 2018). For example, the GDM A geographical detector was used to detect the influence of annual and seasonal factors on the spatial-temporal characteristics of surface water quality (Wang et al., 2018). Other examples are the application of the GDM to examine Moreover, the driving factors' influences factors influencing on regional energy-related carbon emissions (Zhang and Zhao, 2018) and to examine the effects of socioeconomic development on fine particulate matter (PM2.5) in China (Zhou et al., 2018) were examined by the geographical detector technique. In the current study, the GDM is method was used to detect the impact of nine variables and their interactions on the variations of ACIS and cloud parameters over land and ocean. The advantages of using the GDM in this approach are (1) stratified independent variables enhance the representation of a sample unit, so it has higher statistical accuracy than other models with the same sample size; (2) the use of a q-statistic value can afford a higher level of explanatory power, but does not require the existence of a linear relationship between independent and dependent variables; (3) the geographical detector GDM can determine the true interaction between two variables and is not limited to pre-established multiplicative interactions (Wang et al., 2010); (4) the use of a geographical detector the GDM does not need to consider the collinearity of multiple independent variables (Wang et al., 2010).

460

465

470

## 4 Results and Discussion

### 4.1 Spatial distribution and correlation analysis of AOD and cloud parameters

The spatial variations of the AOD and the cloud properties (CER, COT, CF, CTP and LWP) over the study area, averaged over the years 2008-2022, are presented in Fig. 4. Figure 4(a) shows a large difference between the AOD over land and ocean, with the highest values over the northern part of the

475

YRD (averaged AOD larger than 0.5), and the lowest values over the southwestern part of the ECS (<0.1); the AOD decreases gradually from land to ocean. The spatial distributions of the CER, COT, CF, CTP and LWP over the YRD and ECS in Figs. 4(b)-(f) shows that for each of them there is a distinct difference between those over land and over ocean both as regards the values and the spatial variation.

480 Over the ECS, the CER is largest in the south and decreases toward the north of this area and the values are overall substantially larger than over the YRD, where the CER varies somewhat and decreases from north to south. The variation of the CER with AOD over the YRD is opposite to what would be expected, which will be discussed in Sect. 4.2. The COT also varies somewhat over the YRD, but, contrary to the CER, COT increases from north to south. Over the ECS, the COT is generally lower than over the YRD, 485 with the highest values in the [northwest](#)<sup>NW</sup> which gradually decrease toward the [SW](#)<sup>southwest</sup>. Clearly, the CER is higher and the COT is lower over the ECS than over the YRD.

The spatial distributions of CF, CTP and LWP are clearly different. Over the ECS, CF increases from the [SW](#)<sup>southwest</sup> to the [NW](#)<sup>northwest</sup>, opposite to the variations of the CTP and the LWP which are lower in the north of the ECS than in the south. Over ocean the clouds are generally lower (higher CTP) than 490 over land, and CTP varies over the study area with the highest values over land, in the north. Over the YRD, the spatial patterns of the CF and CTP are opposite, with CF increasing from south to north and CTP decreasing. Over the YRD, the spatial distributions of COT and LWP are similar with higher values toward the south. Over the ECS, the LWP varies with the lowest values in the [NW](#)<sup>northwest</sup> and the highest values in the south. The high values of the CER and CF over the ECS could be due to the 495 dominance of sea spray aerosol, the high hygroscopicity of which makes these particles very efficient CCN. [The influence of different factors on the sensitivity of cloud parameters to aerosol and the adjustments are discussed in the following sections, based on both statistical methods and the application of the GDM.](#)

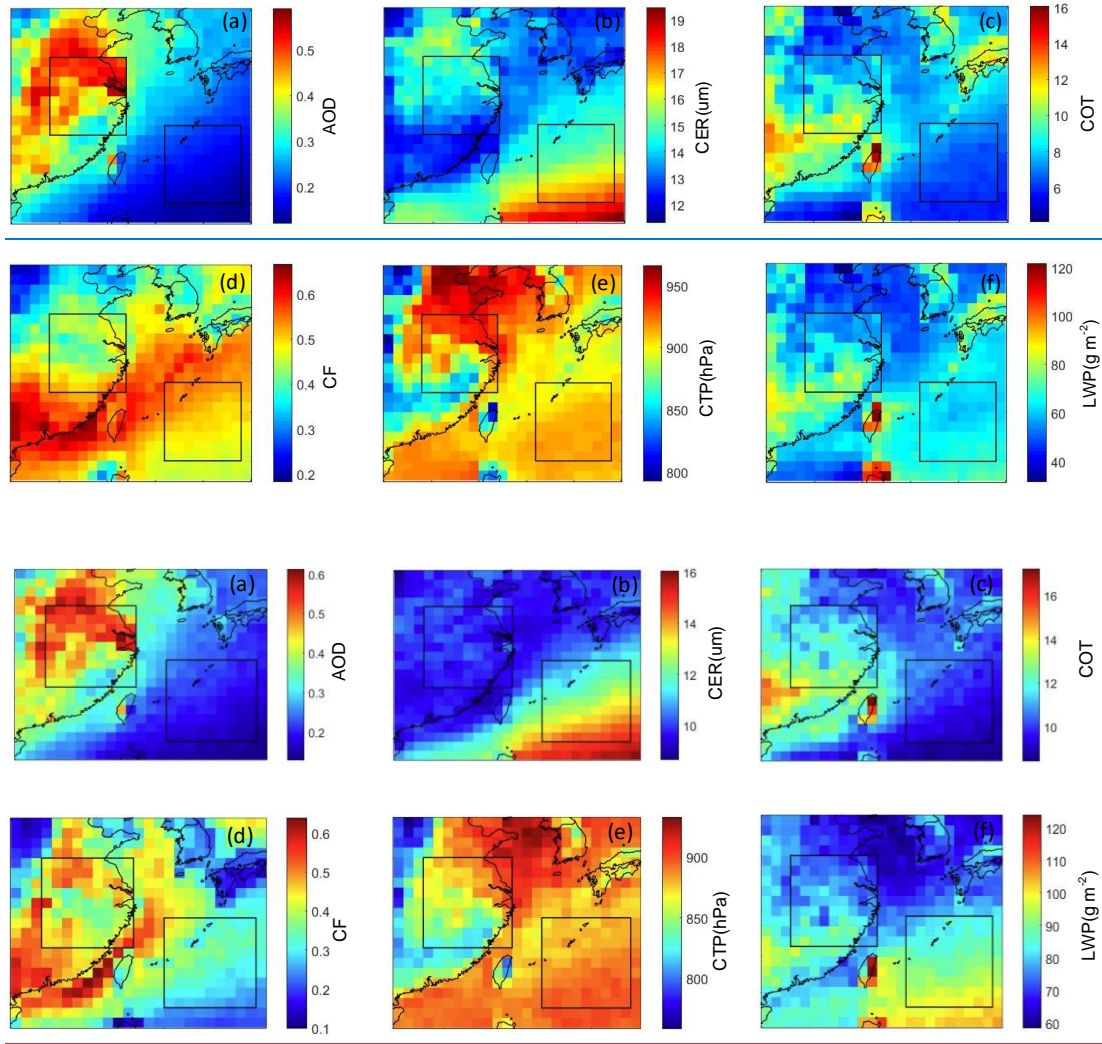


Figure 4. Spatial distributions of AOD (a), CER (b), COT (c), CF (d), CTP (e) and LWP (f), averaged over the years 2008 – 2022, over the study area, with the YRD and ECS marked by the squares.

#### 4.2 Sensitivity of ACI estimates for CER to AOD for the whole LWP regime

Equation Eq. (1) shows that the value of the ACI, the sensitivity  $S$  of CER to AOD is determined by the slope of a linear fit to a log-log plot of CER versus AOD. To investigate the ACI, we used correlated data pairs for 15 years and the data was binned in AOD intervals with a bin width of 0.02, and the CER data in each AOD bin were averaged. Logarithmic plots of the averaged CER data versus AOD over the YRD and the ECS are presented in Figure 5. Figures 5(a) (YRD) and 5(b) (ECS) show different regimes for the variation of the CER with the AOD over the YRD and the ECS. The first regime, for  $AOD \leq 0.05$ , shows the increase of CER with AOD over both regions, followed by a variable CER over the YRD and a gradually stronger decrease over the ECS for AOD between 0.05 and 0.1. In view of this variability and the uncertainty of AOD of  $\pm (0.05 + 15 \%)$  over land and  $\pm (0.03 + 5 \%)$  over ocean (Levy et al.,

2013), ~~the ACIS~~ will not be investigated for  $AOD < 0.1$ . For higher AOD, ~~the CER / AOD relation~~ changes for AOD around 0.3. Thus, the second regime is selected as the part of the CER vs AOD relationship where ~~for~~ AOD varies between 0.1 and 0.3. In this AOD regime, the CER fluctuates a little with AOD over the YRD (Figure 5(a)) ~~but the CER values remain within the standard deviation and S is close to 0 (no the expected discernible Twomey effect) is not observed~~. In contrast, over the ECS the CER clearly decreases with AOD ~~for AOD~~ increasing from 0.1 to 0.3 (Figure 5(b)), in good agreement with expectation based on the Twomey effect, and the correlation between CER and AOD is high with  $R=0.99$  and statistically significant. Note however, that no selection was made for LWP and the condition of constant LWP was not fulfilled. This will be further discussed in Section 4.3.

In the third regime, where  $AOD > 0.3$ , CER increases with increasing AOD over the YRD, with correlation coefficient  $R=0.79$ . In contrast, over the ECS the CER does not significantly change with increasing AOD for  $AOD > 0.3$  (~~very small S~~). However, the large uncertainty in the bin-averaged CER in this AOD regime, increasing with increasing AOD, indicates a very variable ~~ACIS~~ between high-AOD events which on a statistical basis cannot be further analysed and likely depends on the type of aerosol present during each event and the meteorological conditions. The reason for the ~~positive relationship increase of -between CER and with increasing AOD (S positive)~~ over the YRD may be similar to that described by Feingold et al. (2001), i.e., in the presence of a large number of aerosol particles (~~CCN~~) competing for a limited amount of water vapor, only a subset of aerosol particles is activated. Once activated, these particles continue to grow faster, thus preventing water vapor from condensing onto smaller aerosol particles that are less susceptible to activation. As a result, the amount of available water vapor is distributed over a subset of aerosol particles which thus become cloud droplets with relatively large CER and the CER in turn increases with further increasing AOD (Liu et al., 2017). The ~~CER sensitivity response of CER~~ to AOD is stronger over the ECS ( $0.1 < AOD < 0.3$ ) than over the YRD ( $AOD > 0.3$ ). It is anticipated that during the relatively low AOD over the ECS ~~during-in~~ AOD regime 2 ( ~~$0.1 < AOD < 0.3$~~   ~~$AOD 0.1 0.3$~~ ) the aerosol number concentration is dominated by sea spray aerosol particles (de Leeuw et al., 2011) which are hygroscopic and thus provide good CCN, while over open ocean also the ~~relative humidity RH~~ is generally high. Hence the available water vapor will be readily distributed over all CCN, resulting in the decrease of the CER and a strong correlation with AOD. Further, the AOD over open ocean does not reach high values in the absence of continental influence,

even in very high wind speeds the AOD does not exceed 0.2 (Huang et al., 2010; Smirnov et al., 2012).

Hence AOD higher than 0.2 over the ECS is influenced by long-range transport of aerosol produced over

545

land with lower hygroscopicity, and thus lower susceptibility to act as CCN, which explains the breakdown of the Twomey effect over the ECS for elevated AOD. In fact, the data in Figure 5(b) show that the CER/AOD relationship starts to flatten for AOD ~0.2 and is flat for AOD larger than ~0.3.

Overall, Figure 5 shows that the Twomey effect is clear in the second AOD regime over the ECS and [the anti-Twomey effect](#) in the third AOD regime over the YRD. For this reason, the further analysis focuses

550

on the [aci-ACI](#) over the ECS for AOD between 0.1 to 0.3, and over the YRD for AOD > 0.3.

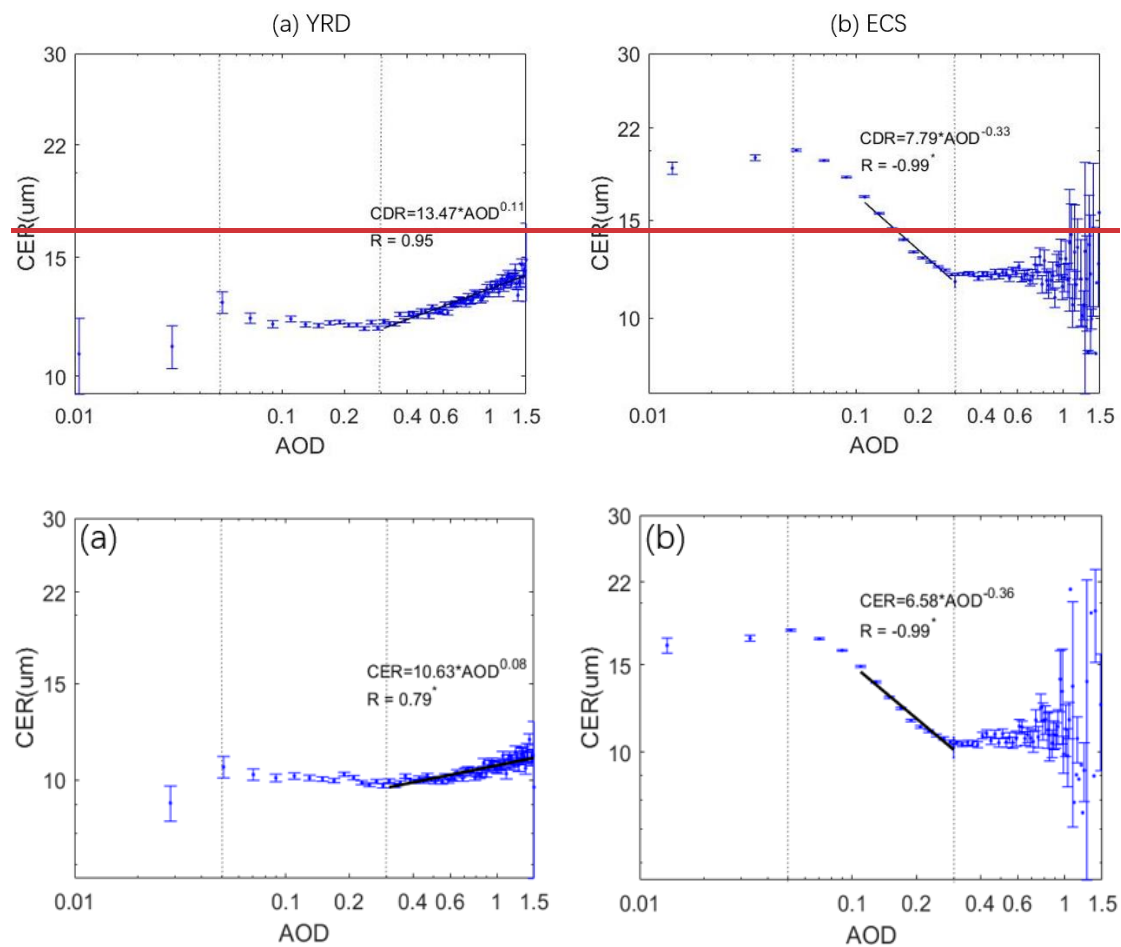
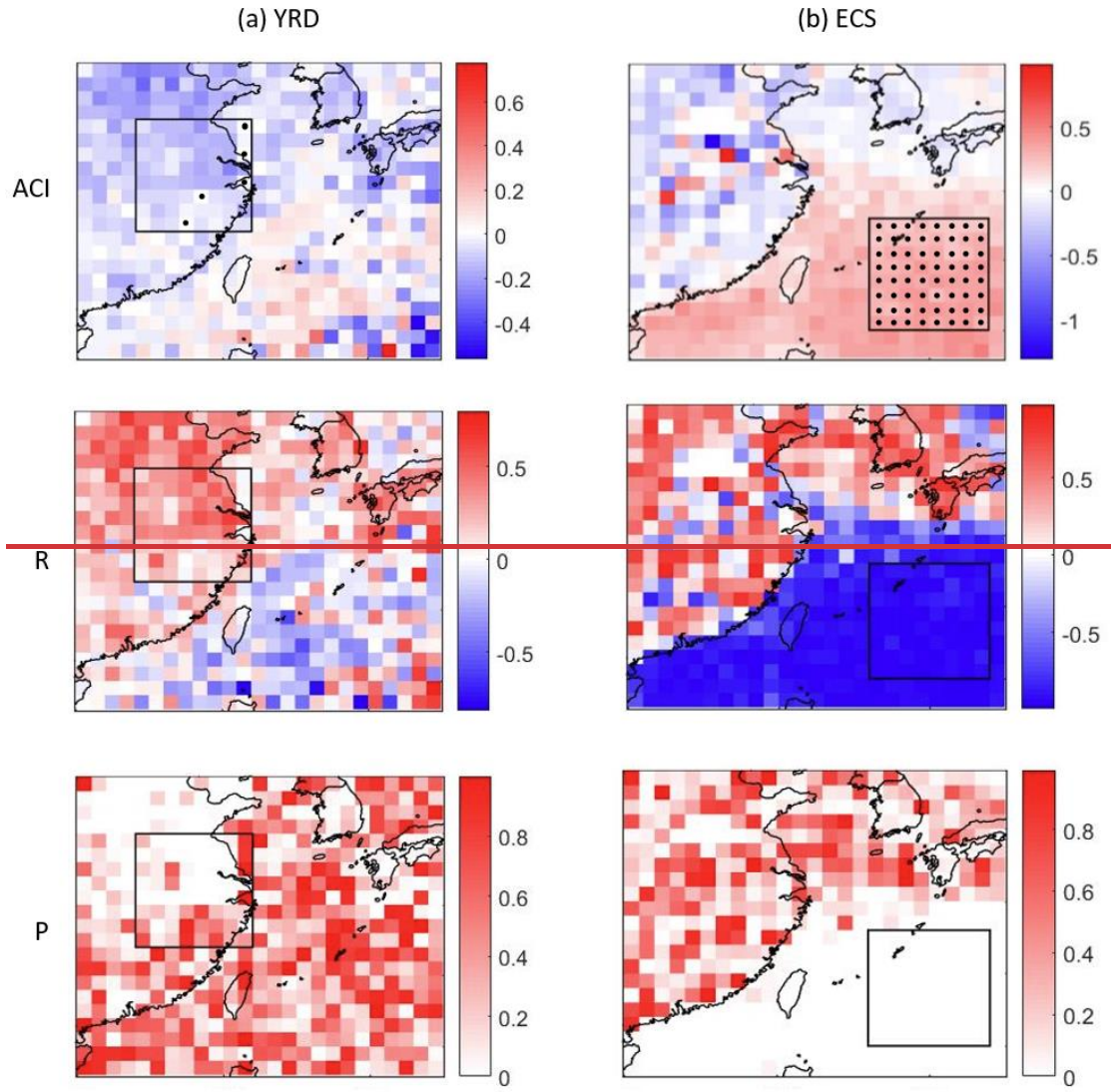


Figure 5. Variation of CER with AOD over the YRD (a) and [the ECS](#) (b). Here all CER data were averaged in AOD bins, from 0.0 to 1.5 with a step of 0.02. Note that the data are plotted on a log-log scale. The lines for the YRD data for AOD>0.3 and for the ECS data for 0.1<AOD<0.3 represent least-square fits to the binned data, and the resulting relations are presented in each figure. The marker \* at the top right corner of the R value indicates that the correlation is statistically significant with  $p < 0.0501$ . The thin vertical lines indicate the AOD regimes as explained in the text.

555

To study the spatial variation of [the ACIS](#) over the study area, [the ACIS in each grid cell](#) has been

560 calculated in each grid cell by application of Equation Eq. (1) to all observations over the YRD for which  
AOD>0.3 and to all observations over the ECS for which  $0.1 < \text{AOD} < 0.3$ . The results are plotted in  
Figure 6, which shows maps of the ACIS, the correlation coefficient R between CER and AOD and the  
statistical P-value for each grid cell over the study area. Figure 6(b) shows that the ACI over the ECS,  
for the second AOD regime (0.1-0.3), S is positive~~negative~~, with large negative correlation coefficients  
565 ~~(-0.7866 to -0.9998)~~ which mostly are statistically significant ( $p < 0.01$ ). These results show the good  
correlation between CER and AOD, consistent with the cloud albedo effect~~theory of the first AIE~~. In  
contrast, over the YRD, for the third AOD regime ( $>0.3$ ), the ACIS is mostly negative~~positive~~ and the  
correlation between CER and AOD is positive, i.e. high aerosol loading results in larger CER for  
AOD>0.3, as was also concluded from Figures 5(a) and (b). The data in Figure 6(a) also show that, the  
570 negative over the YRD, S is largest over the CER/AOD relation is strongest in the part of the selected  
YRD region area to the north of Shanghai but R is relatively small~~weak~~ (0.11 to 0.6335) and for the  
majority of the cells the correlations are not statistically significant ( $p \sim 0.1$  or larger). In the part of  
the selected YRD region sSouth of Shanghai the correlations are small and not statistically significant.  
The observed anti-Twomey effect of aerosols over the YRD has also been reported in earlier publications  
575 such as Jin and Shepherd (2008), Yuan et al. (2008) and Liu et al. (2017). Factors influencing the  
relationship between AOD and cloud parameters have been reported in the literature, such as hygroscopic  
effects (e.g., Qiu et al., 2017), atmospheric stability, cloud dynamics, cloud height (Shao and Liu, 2005)  
and land cover type (Jin and Shepherd, 2008; Ten Hoeve et al., 2011). The effects of competing  
mechanisms and their possible influence on the observed response of CER to high AOD in the YRD will  
580 be further discussed in the following sections.





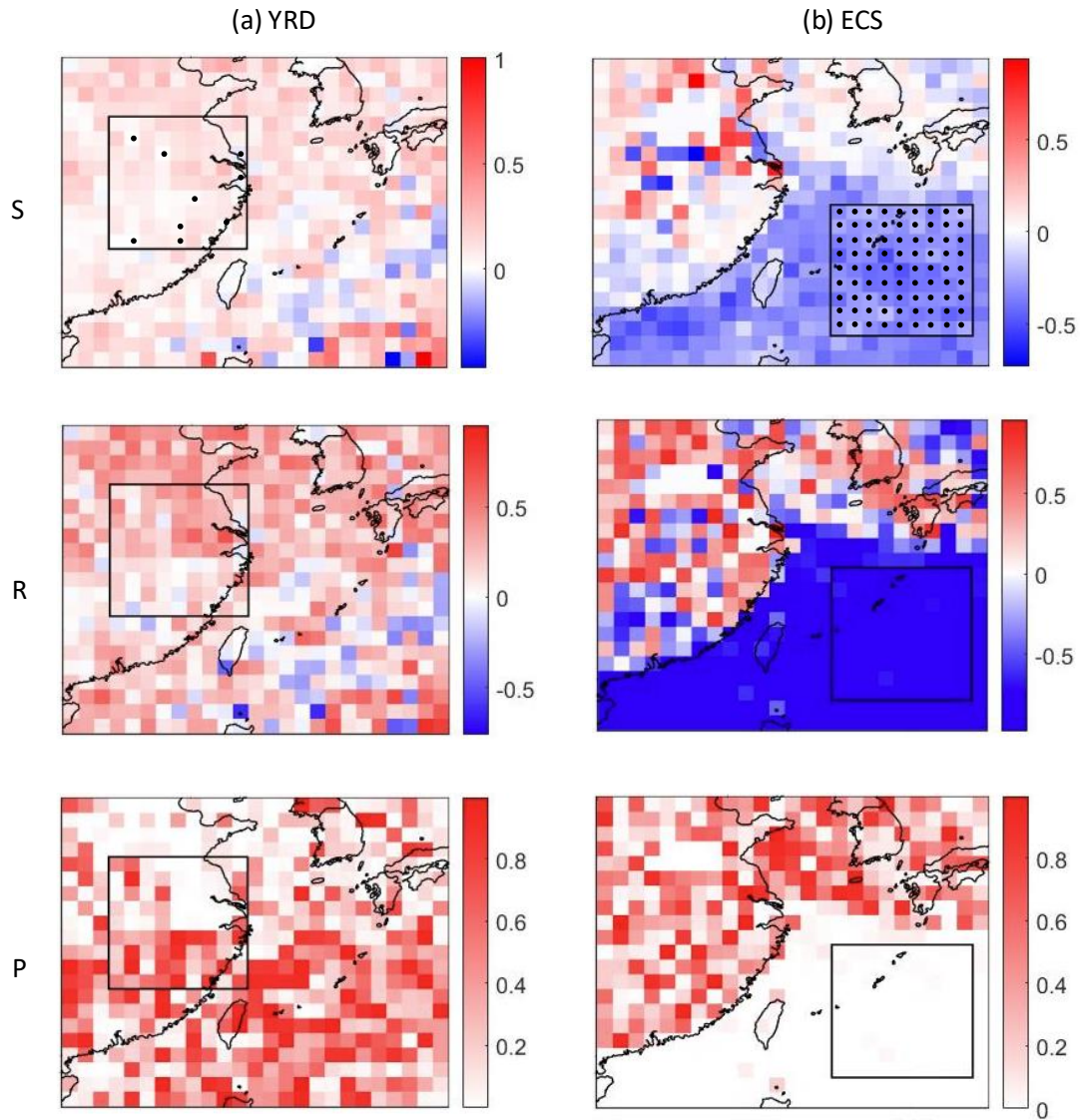


Figure 6. Using the AOD as a proxy for ~~–aerosol concentrations~~CCN, estimates of the ~~ACI for CER~~ sensitivity to aerosol (S) were calculated for each grid point in both study areas. Maps of the spatial distributions of the ~~ACIS~~, the correlation coefficients and the statistical P-values in each grid point are presented in Figure (a) for over the YRD (left column, Figure 6(a)) for the AOD regime with AOD>0.3 and in Figure (b) over the ECS (right column, Figure 6(b)) for the AOD regime with 0.1<AOD<0.3 (right column, Figure 6b). ~~ACIS~~, R and P-values are color coded following the color bars at the right of each figure. The black solid dots in the top figures (S), indicate that the ~~ACIS~~ value is ~~positive/negative~~ in the grid point over the YRD and ECS.

#### 4.3 Sensitivity of CER to AOD ~~ACI estimates for CER for different~~ stratified by LWP regimes

In the data presentation and discussion of S in Section 4.2, the condition of constant LWP (Equation 1) was not considered. Because constant LWP is a condition for the application of Eq. (1) and the occurrence of ~~to the cloud albedo effect, was not considered.~~ calculate ACI, in In this Section –the effect of LWP on S will be further investigated. To this end, the condition of constant LWP is approached by

595 ~~stratifying considering LWP into~~ five LWP intervals, each with a width of  $40 \text{ g m}^{-2}$ , ~~for the LWP the~~ range  
of  $[0 \text{ g m}^{-2}, 200 \text{ g m}^{-2}]$ . ~~The ACIS in the whole area~~ was calculated ~~over the YRD and the ECS~~, for each  
LWP interval using Eq. ~~uation~~ (1) for all observations over the YRD for which  $\text{AOD} > 0.3$  and ~~for~~ all  
observations over the ECS for which  $0.1 < \text{AOD} < 0.3$ . The results are presented in Table ~~23~~, together with  
the corresponding correlation coefficients R ~~for the relation~~ between ~~the~~ CER and AOD in the relevant  
600 AOD regimes. ~~The significance of these correlations was determined by using the student's t test, i.e. the~~  
~~results are statistically significant when the p value is smaller than 0.01, where p is defined as the~~  
~~probability of obtaining a result equal to or "more extreme" than what was actually observed.~~ The data  
in Table ~~2-3~~ show that over the ECS, ~~the ACI estimates are~~ S is ~~negative positive~~ and statistically  
significant for all four LWP ranges between  $40$  and  $200 \text{ g.m}^{-2}$ , ~~and~~ ~~The sensitivity becomes stronger as~~  
605 ~~LWP increase with~~ increasing LWPes, i.e., S changes from  $-0.197$  (LWP  $40\text{-}80 \text{ g.m}^{-2}$ ) to  $-0.462$  in the  
highest LWP range ( $160\text{-}200 \text{ g.m}^{-3}$ ), with corresponding R of  $-0.98$  to  $-0.99$ . Thus, the magnitude of the  
LWP has a substantial influence on the ~~aerosol albedo~~ effect ~~on the ACI~~. Over the YRD, ~~the ACIS~~ is  
~~positive and statistically~~ significant in the first three LWP regimes, with ~~values the ACI~~ varying between  
 $-0.0640$  and  $-0.103$  ~~and~~ ~~with~~ a correlation R between  $0.5776$  and  $0.8196$ . These data show that, ~~in~~  
610 ~~contrast to the ECS~~, over the YRD the ~~variation of the~~ LWP effect ~~has little influence~~ on ~~the aci~~ S ~~ACI is~~  
~~smaller than over the ECS~~ and, ~~in contrast to the ECS~~, over the YRD ~~thus~~ the magnitude of the LWP has  
little influence on the ~~strength of the ACI albedo effect~~.

In summary, the data show that both over the ECS and the YRD the relationships between the CER and  
the AOD are significant, but for different LWP intervals ( $[0 \text{ g m}^{-2}, 120 \text{ g m}^{-2}]$  over the YRD and  $[40 \text{ g m}^{-2}$   
615  $^2, 200 \text{ g m}^{-2}]$  over the ECS) and for different AOD regimes ( $0.1 < \text{AOD} < 0.3$  over the ECS and  $\text{AOD} > 0.3$   
over the YRD), and that the ~~aci~~ ~~ACI~~ CER-AOD relation follows the Twomey effect over the ECS and the  
anti-Twomey effect over the YRD.

~~The variation of S with changes in LWP indicates that the condition of constant LWP is not truly satisfied:~~  
~~if the data would be stratified according to smaller LWP intervals (quasi-constant LWP, Ma et al., 2018),~~  
620 ~~S would likely vary more smoothly with LWP. As mentioned in the Introduction, LWP is not directly~~  
~~retrieved but calculated form CER and COT and thus also the calculation of S is to some extend affected~~  
~~by LWP. We further note the results by Ma et al. (2018), i.e. the slope of CER versus AI (comparable to~~  
~~S in this paper) varies little with LWP, with positive values over land and negative values over ocean and~~

thus behaves similar to the data in Table 3 for YRD and ECS.

625 In the following study on the effects of the AOD and different cloud and meteorological properties on  
~~the ACIS and adjustments, using the GDM,~~ these differences will be taken into account, i.e. over the  
 YRD only data with AOD > 0.3 and LWP in the range from 0 to 120 g m<sup>-2</sup> will be used and over the ECS  
 only data with AOD in the interval [0.1, 0.3] and LWP in the range from 40 to 200 g m<sup>-2</sup> will be used.

630 **Table 23. ACIS Estimates of S, computed using Eq. (1), and correlation coefficients R between the CER and  
 -AOD, relationships in five different stratified by LWP, -LWP intervals computed using Equation (1) over  
 the ECS for 0.1 < AOD < 0.3 and over the YRD for AOD > 0.3. Statistically significant data points are indicated  
 with \* (p value < 0.01).**

		ECS (0.1 < AOD < 0.3)		YRD (AOD > 0.3)	
LWP	ACI	R	ACI	R	
0-40	-0.13	0.99*	-0.12	0.91*	
40-80	0.17	-0.98*	-0.13	0.96*	
80-120	0.35	-0.99*	-0.10	0.76*	
120-160	0.41	-0.99*	0.01	-0.10	
160-200	0.42	-0.99*	0.08	-0.37*	

635

		ECS (0.1 < AOD < 0.3)		YRD (AOD > 0.3)	
LWP (g m <sup>-2</sup> )	ACIS	R	ACIS	R	
0-40	-0.10	0.94*	-0.08	0.63*	
40-80	-0.19	-0.98*	-0.10	0.81*	
80-120	-0.38	-0.99*	-0.06	0.57*	
120-160	-0.41	-0.99*	-0.03	-0.11	
160-200	-0.46	-0.98*	-0.14	-0.42*	

#### 4.4 Behaviour of CER and other cloud properties with the increase of AOD

Scatterplots of the CER versus other cloud properties (COT, CF and CTP), with AOD as third parameter  
 (color-coded), are presented in Figure 8, over the ECS and the YRD, are presented in Figure 87. Over  
 the ECS, the CER and CTP decrease (the cloud top height increases) with the increase of AOD, and the  
 640 COT and CF increase. The increase of AOD indicates an increase of the aerosol concentration and thus  
 potentially the number of CCN, which in turn, upon activation, results in the increase of the number of  
 cloud droplets and thus an increase of the COT. The positive correlation between COT and AOD over  
 the ECS suggests that the thicker clouds contain more water droplets and are formed in a more polluted  
 atmosphere, which, as discussed in Section 4.2, results from the influence of long-range transport of

645 aerosol produced over land on the aerosol burden over ocean. But at the same time, as Figure- 87(a) shows, CER decreases with increasing AOD, resulting in the increase in cloud albedo and thus also in the increase of COT. The increase of cloud top height with AOD indicates that both the horizontal and vertical expansion of the clouds are also enhanced. These observations are in agreement with the strong correlation between aerosol loading and cloud vertical development for convective clouds over the North  
650 Atlantic reported by Koren et al. (2005).

In contrast to the situation over the ECS, over the YRD the increase of AOD results in an increase of the CER and CTP (the cloud top height decreases), and a decrease of the COT. These observations are consistent with those proposed by Liu et al. (2017) in the same study region. The decrease of the CF with increasing AOD could be explained as follows. Due to the high concentration of smoke particles over the  
655 YRD (Shen et al., 2021), aerosol particles absorb solar radiation which results in local heating of the aerosol layer and cooling of the surface (Li et al., 2017). This in turn stabilizes the temperature profile and reduces the relative humidity and surface moisture fluxes (evapotranspiration) (Koren et al., 2008) and thus also cloudiness. Reduced cloud cover exposes greater areas of the aerosol layer to direct irradiation from the Sun and therefore produces more intense heating of the aerosol layer, further  
660 reducing cloudiness (Koren et al., 2008). It is noted that this process is different from that proposed by Liu et al. (2017), i.e. that the CF increases with increasing AOD in polluted and heavily polluted conditions ( $AOD > 0.3$ ). In the study of Liu et al. (2017), the LWP range was not constrained, i.e. ~~the~~ aerosol-cloud interaction ~~relationship~~ was studied considering the whole LWP range. The data presented in Table 23, shows that ~~the ACIS~~ significantly changes between ~~different LWP regimes, i.e. for~~ the three  
665 LWP intervals between 0 and  $120 \text{ g m}^{-2}$ ; ~~the where ACIS~~ is ~~negative positive~~ (anti-Twomey effect) and for larger LWP it is ~~positive negative~~ but statistically not significant. Figure 9-8 shows that CER and CTP substantially increase, whereas COT and CF decrease with increasing AOD in the two LWP intervals between  $40\text{-}120 \text{ g m}^{-2}$ . However, in the other three LWP intervals the relationships between these cloud parameters and AOD are not evident. The different explanations offered here and in Liu et al. (2017) may  
670 be related to the different aerosol and cloud ~~properties~~ data sets used by Liu et al., (2017) and in the current study. On the one hand, the data sets have a different spatial resolution and cover a different time period. The dataset used in the study of Liu et al. (2017) are MYD04 Level 2 Collection 5 and MYD06 Level 2 Collection 5 in the period from 2007 to 2010. During that period the AOD over the YRD was at

675 a maximum and decreased substantially in later years (Liu et al, 2021; de Leeuw et al., 2022; 2023). On the other hand, in the study of Liu et al. (2017), the MODIS-retrieved AOD was averaged over an area with a radius of 50 km from the CALIOP target and the MODIS-retrieved cloud data were averaged within a radius of 5 km from the CALIOP target. Hence the AOD and cloud parameters were not representative for the same area, in particular in cases with inhomogeneous spatial distributions.

680

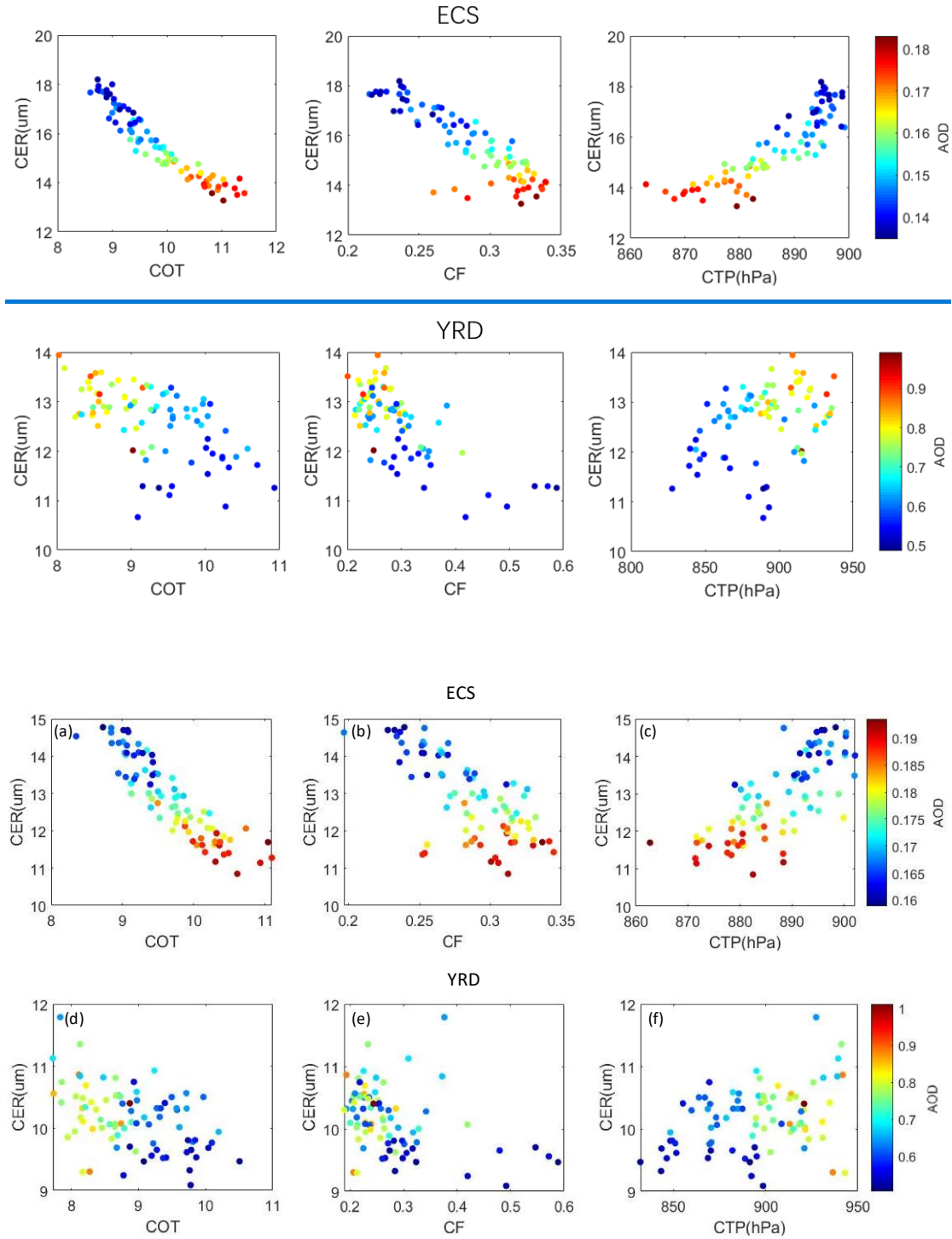
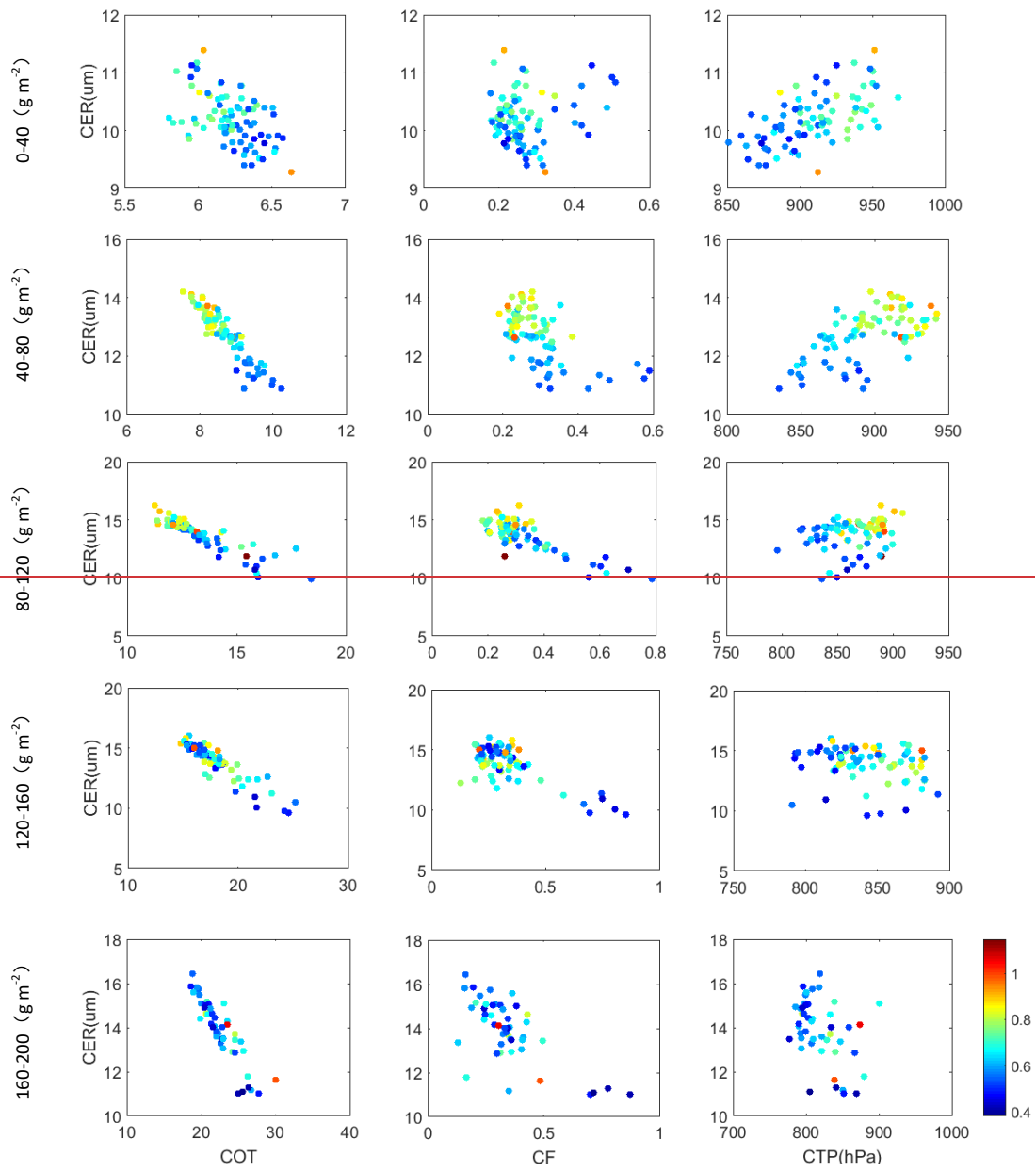
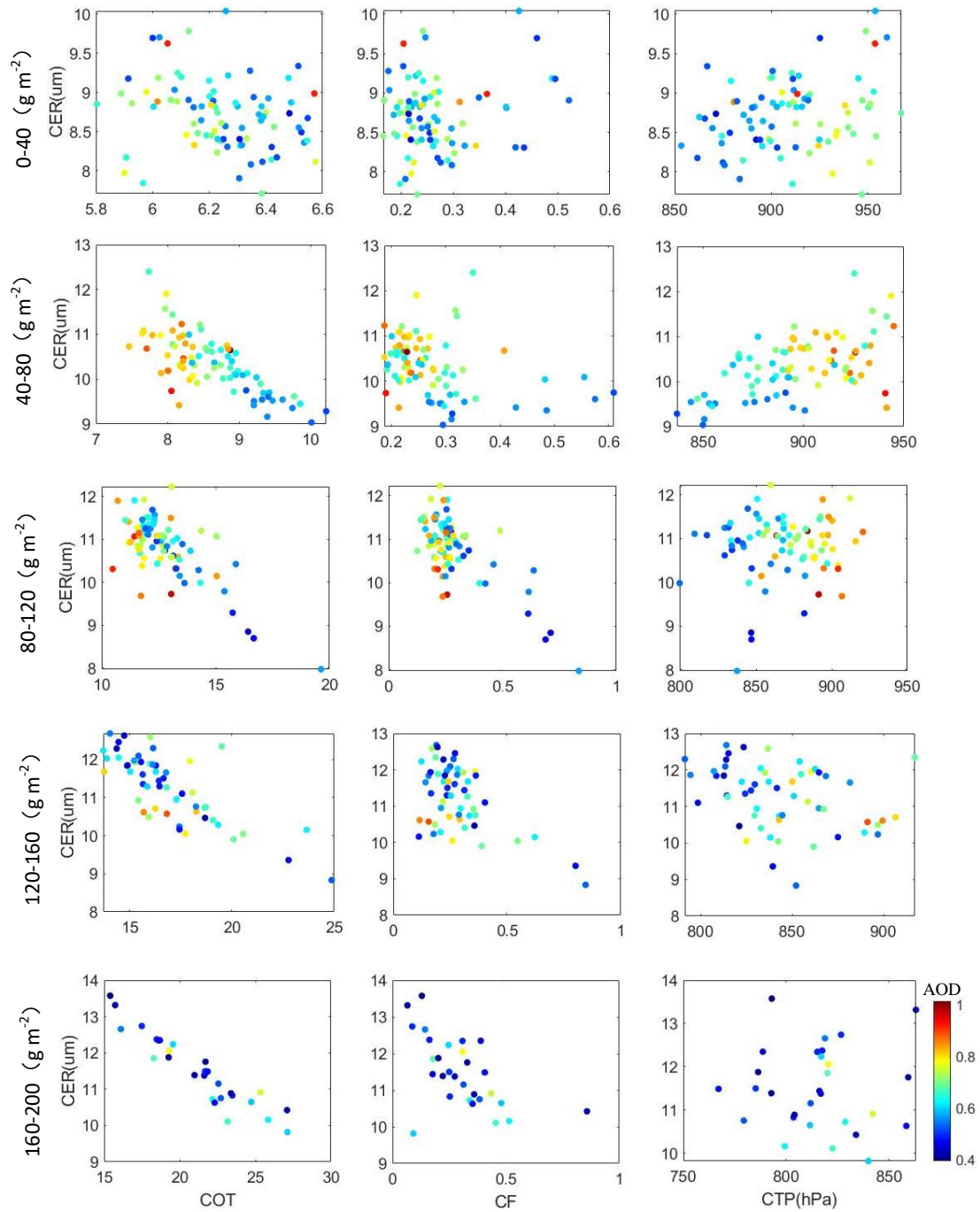


Figure 87. Scatterplots of CER versus other cloud parameters (COT, CF and CTP; left to right) over the ECS

(top row) and the YRD (bottom row), with AOD as third parameter, color coded following the scale at the right.



685



**Figure 98.** Scatterplots of CER versus other cloud parameters (COT, CF and CTP; left to right) over the YRD, for ~~three~~ five different LWP intervals between 0 and 200  $\text{g m}^{-2}$ . The AOD for each grid point is color coded following the scale at the right.

690 **4.5 Behaviour of CER and AOD in different meteorological conditions**

Scatterplots of the CER versus AOD over the ECS and the YRD, with meteorological factors (LTS, RH, PVV) (color coded) as third parameter, are presented in Figure 109. Over the ECS (Figure 109(a)), the AOD is inversely related to LTS, whereas the CER increases with increasing LTS. This observation is

different from the findings of Saponaro et al. (2017) who reported that there is no significant influence  
695 of atmospheric stability (LTS) on the relationship between CER and AOD. Likewise, the AOD is  
inversely related to RH whereas CER increases with increasing RH. These two observations indicate that  
RH and LTS have a similar effect on the relationship between AOD and CER. In contrast, with the  
increase of PVV, the AOD becomes larger but the CER becomes smaller. The CER vs AOD curves show  
that, overall, the meteorological conditions do not change the functional relationship between AOD and  
700 CER, but quantitatively they do have an effect. The change of meteorological conditions plays an  
important role in the variation of CER. ~~In addition, Figure 10b shows that, over the ECS, with the increase  
of the aerosol concentrations, the number of cloud condensation nuclei also increases, so the same  
amount of water vapor is distributed over a larger number of cloud droplets resulting in smaller cloud  
droplets. Hence, the interaction between AOD and CER over the ECS is in agreement with the Twomey  
cloud albedo effect.~~

705 ~~Cloud properties as a function of AOD for two different LTS conditions over the YRD are presented in  
figure 10d, i.e. for low LTS, with a mean value of 13.27 representing an unstable atmosphere; and for  
high LTS, with a mean value of 15.23 representing a stable atmosphere. In unstable atmospheric  
conditions the CER is larger than in stable conditions, and in both unstable and stable conditions CER  
increases with AOD. The larger CER in unstable conditions may be due to better vertical mixing of both  
aerosol particles and water vapor (Liu et al., 2017).~~

715 ~~The effect of relative humidity (RH, at 750 hPa) on the relationship between the cloud properties and  
AOD is evaluated by dividing the data into two equally sized subsets for high and low RH, and the mean  
relative humidity values for each subset are calculated. In high relative humidity conditions (57%) the  
CER is much larger than in low relative humidity conditions (48%), as shown in Fig. 10e.~~

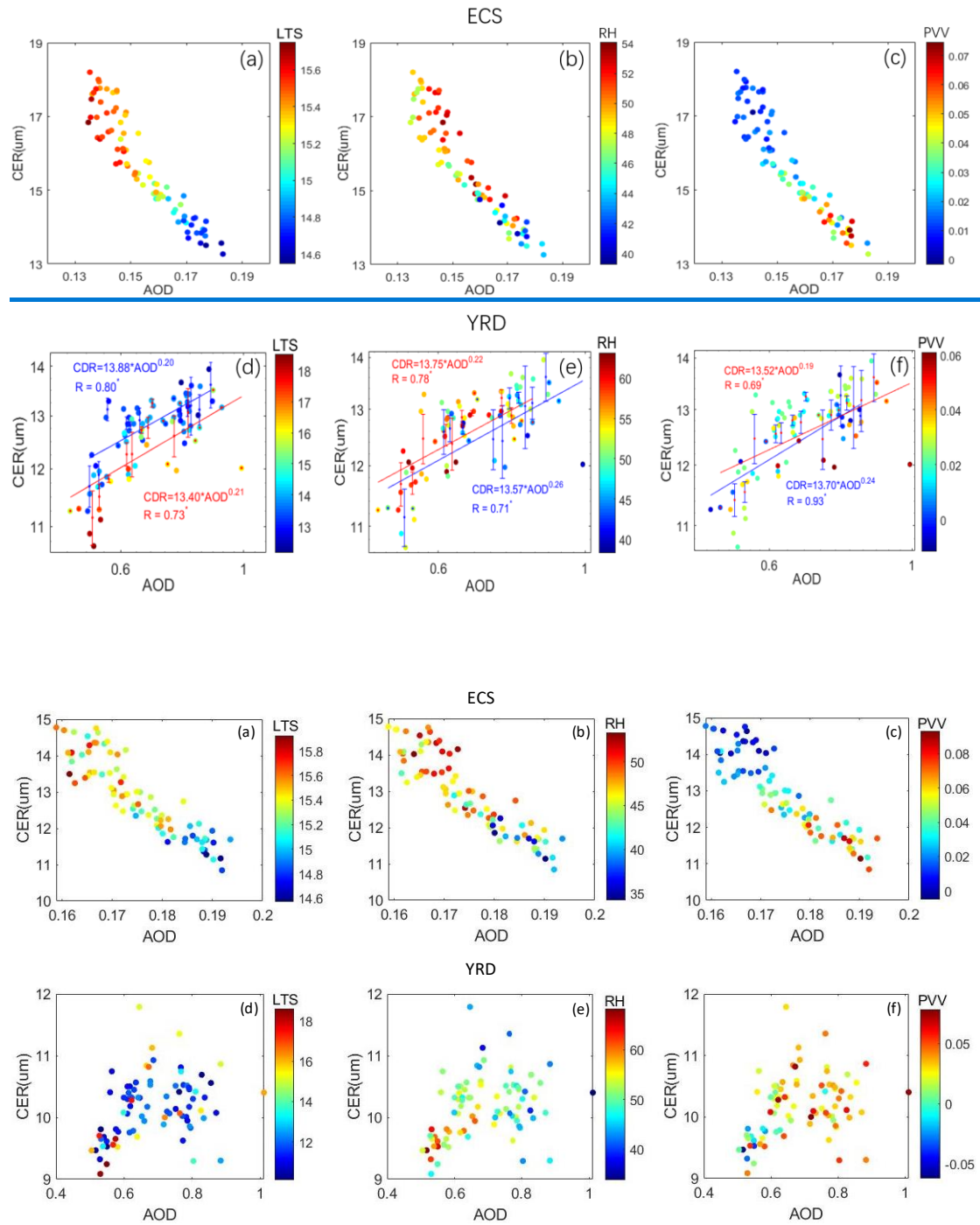
~~Different from the situation over the ECS, over the YRD the effect of meteorological conditions on the  
CER is weak as shown in Figures 9(d)-(f). RH and PVV shows have an inverse role in effect on the  
relationship between AOD and CER. There is no significant influence of atmospheric stability (LTS) on  
the relationship between CER and AOD as suggested by Saponaro et al. (2017). Overall Therefore,  
720 aerosol concentration plays a dominant more important role in the effects of different factors on CER over  
the YRD.~~

~~The effect of vertical velocity (PVV) on the CER in polluted and heavily polluted conditions is weak. In~~



general, the influence of aerosol concentration (AOD) on the CER is larger than that of meteorological conditions, although the combined effect of AOD and meteorological conditions is larger than that of AOD alone (Fig. 7). Therefore, aerosol concentration plays a dominant role in the effects of different factors on CER.

725



730

**Figure 109.** Scatterplots of CER versus meteorological parameters (LTS, RH and PVV; left to right) over the ECS (top row) and the YRD (bottom row). The AOD for each grid point is color coded following the scale at the right. The lines in the bottom row (YRD) present the least square fits for low and high LTS, RH and PVV, respectively, as described in the text, and the resulting relations are presented in each figure. The marker \*

at the top right corner of R-value denotes statistically significant if  $p < 0.05$ .

## 735 4.6 Application of the Geographical-geographical detector model-method analysis

### 4.6.1 Factor detector analysis

The GDM factor detector module was used to analyze the influence of 9 factors (aerosol/AOD, cloud and meteorological conditions/parameters) on ACI-S over the YRD and the ECS, for the conditions summarized at the end of Section 4.3. These factors are summarized in Table 34, together with q, i.e. the explanatory power of that factor to S q-values (Equation Eq. 2), over the ECS and the YRD. The data in Table 3-4 show that the influences of the 9 proxy variables on S are rather weak and not statistically significant. ~~and~~ They can explain only 1%-15% of the variation of S in both target regions. ~~over the ECS, only the influences of the proxy variables CER and CF have some are statistically significant with  $p < 0.1$ .~~ Over the YRD, the variables CER, LWP, CF, RH and LTS all exert all have some significant impacts on ACI-CER but with small statistical significance (at the  $p < 0.1$ ) level. In addition to the weak statistical significances, ~~however,~~ also the q-values show that the influences of the 9-se variables on the ACI values S is are rather weak and can explain only 10%-22% of the variation of the ACIS. Furthermore, in neither of the two regions the influence of the proxy variables AOD, COT, CTP and PVV is statistically significant at the 0.1 level.

750 **Table 34.** q values for factors which may influence ACI-S over the ECS and the YRD, evaluated for data collected in the period from 2008-2022.

	Aerosol parameter	Cloud parameters					Meteorology parameters			
	AOD	CER	COT	LWP	CF	CTP	RH	LTS	PVV	
ECS	0.06	0.14 <sup>z</sup>	0.16	0.10	0.16 <sup>z</sup>	0.10	0.04	0.04	0.09	
YRD	0.06	0.10 <sup>*</sup>	0.05	0.22 <sup>*</sup>	0.21 <sup>*</sup>	0.05	0.13 <sup>*</sup>	0.16 <sup>*</sup>	0.04	

Study Area	Aerosol parameter	Cloud parameters					Meteorological parameters			
	AOD	CER	COT	LWP	CF	CTP	RH	LTS	PVV	
ECS	0.07	0.06	0.06	0.10	0.01	0.13	0.10	0.11	0.09	
YRD	0.05	0.09	0.06	0.05	0.04	0.06	0.15	0.09	0.09	

755 Note: <sup>\*\*\*</sup> indicates that the q value is significant at the 0.01 level ( $p < 0.01$ ).

The GDM factor detector module was also used to analyze the influence of the AOD and meteorological parameters ~~factors~~ (RH, LTS and PVV) on adjustments of cloud properties. The results in Table 4.5 show that ~~over the ECS,~~ AOD, ~~LTS~~ and PVV influence all cloud parameters over the ECS except CTP, with q-values which are statistically significant at the 1% level. The ~~high~~ q-values for AOD show that this factor ~~e AOD~~ can explain ~~46.71%~~ (for CF) to ~~81.7%~~ (for CER) of the variation in the cloud parameters considered in this study, and PVV can explain 47% (for CF) and 47% (for COT), which both are similar to the explanatory power of AOD, to 70% (for CER) of the variation in the cloud parameters. For LTS and RH, the q-values for CER are statistically significant but with smaller explanatory power than for AOD and PVV. In contrast, the q-value of LTS for LWP is statistically significant and not much smaller than for PVV, which is substantially more than the explanatory power of the meteorological parameters. Among the meteorological parameters, ~~LTS has the largest influence on cloud parameters and the effect of RH is the smallest.~~

**Table 4.5. q values for factors which may influence cloud parameters over the ECS, evaluated for data collected in the period from 2008-2022.**

	<u>AOD</u>	<u>RH</u>	<u>LTS</u>	<u>PVV</u>
<u>CER</u>	0.87 <sup>***</sup>	0.36 <sup>***</sup>	0.75 <sup>***</sup>	0.69 <sup>***</sup>
<u>COT</u>	0.83 <sup>***</sup>	0.48 <sup>*</sup>	0.79 <sup>***</sup>	0.69 <sup>***</sup>
<u>LWP</u>	0.74 <sup>***</sup>	0.23	0.58 <sup>***</sup>	0.56 <sup>***</sup>
<u>CF</u>	0.71 <sup>***</sup>	0.24	0.56 <sup>***</sup>	0.54 <sup>***</sup>
<u>CTP</u>	0.78	0.54	0.70	0.74

<u>Cloud parameters</u>	<u>AOD</u>	<u>RH</u>	<u>LTS</u>	<u>PVV</u>
<u>CER</u>	0.81 <sup>***</sup>	0.33 <sup>***</sup>	0.44 <sup>***</sup>	0.70 <sup>***</sup>
<u>COT</u>	0.69 <sup>***</sup>	0.40	0.38	0.67 <sup>***</sup>
<u>LWP</u>	0.68 <sup>***</sup>	0.23	0.43 <sup>***</sup>	0.49 <sup>***</sup>
<u>CF</u>	0.46 <sup>***</sup>	0.20	0.09	0.47 <sup>***</sup>
<u>CTP</u>	0.47	0.53	0.18	0.58

Note: \*\*\* indicates that the q value is significant at the 0.01 level ( $p < 0.01$ ). \*\* indicates that the q value is significant at the 0.05 level ( $p < 0.05$ ). \* indicates that the q value is significant at the 0.1 level ( $p < 0.1$ ).

The results from a similar analysis of the data over the YRD (Table 5.6) show that AOD has a statistically significant influence at the 1% level on COT and CF, but with much smaller explanatory power than over the ECS. AOD can explain ~~31.54%~~ of the variation of CER but the statistical significance is small ( $p < 0.1$ ).

Among the meteorological parameters, RH has a statistically significant influence on CTP and can explain 7465% of the variation of the CTP and LTS can explain 4855% of the variation of the LWP and 50% of the variation of the CF with  $p < 0.01$ . The explanatory power for the effects of RH (3732%), LTS (46%) and PVV (1846%) on LWP are substantial but with low statistical significance ( $p < 0.1$ ).

785

**Table 56. q values for factors which may influence cloud parameters over the YRD, evaluated for data collected in the period from 2008-2022.**

	AOD	RH	LTS	PVV
CER	0.54 <sup>±</sup>	0.05	0.41	0.14
COT	0.61 <sup>***</sup>	0.27	0.04	0.19
LWP	0.18	0.37 <sup>±</sup>	0.46 <sup>±</sup>	0.46 <sup>±</sup>
CF	0.33 <sup>***</sup>	0.04	0.48 <sup>***</sup>	0.12
CTP	0.48	0.65 <sup>***</sup>	0.22	0.38

Cloud parameters	AOD	RH	LTS	PVV
CER	0.31	0.25	0.13	0.18
COT	0.61 <sup>***</sup>	0.45	0.12	0.29
LWP	0.16	0.32	0.55 <sup>***</sup>	0.18
CF	0.30 <sup>***</sup>	0.02	0.50 <sup>***</sup>	0.07
CTP	0.50	0.74 <sup>***</sup>	0.32	0.56

Note: \*\*\*indicates that the q value is significant at the 0.01 level ( $p < 0.01$ ).

790

~~\*\* indicates that the q value is significant at the 0.05 level ( $p < 0.05$ ). \* indicates that the q value is significant at the 0.1 level ( $p < 0.1$ ).~~

795

~~In Tables 5 and 6 list q values were given for individual factors, together with p showing the absence of statistical significance in many cases, especially over the YRD, and often the explanatory power is not so high when the significance is low. These data show We find that cloud parameters are seem to be dominated by aerosol effects over the ECS but meteorological influences on cloud parameters predominate over the YRD, as was also concluded from the analysis from “traditional” statistical methods presented in Section 4.5 and these conclusions are which is consistent with the results published by Andersen and Cermak (2015). Among the meteorological parameters, we also find that PVV (with highest q in the three meteorological parameters) predominantly influences on cloud parameters over the ECS. Jones et al. (2009) and Jia et al. (2022) reported that stronger aerosol cloud interactions typically occur under higher updraft velocity conditions. In addition, we find that CTP is mainly affected by RH ( $q = 0.74^{***}$ ) and PVV ( $q = 0.56$ ) over the YRD, as suggested by Koren et al. (2010). Koren et al. The author reported that observed cloud top height correlates best with model pressure updraft velocity and~~

800

relative humidity. To some extent, LTS influences ~~on~~-CER ( $q = 0.44^{***}$ ) and LWP ( $q = 0.43^{***}$ ) over the ECS, while, in contrast, over the YRD LTS predominately influences ~~on~~-CF ( $q = 0.50^{***}$ ) and LWP ( $q = 0.55^{***}$ ) over the YRD. Matsui et al. (2004) and Tan et al. (2017) reported that aerosol impact on CER is stronger in more dynamic environments that feature a lower LTS and argue that very high LTS environments dynamically suppress cloud droplet growth and reduce aci intensity. While strong correlations between AOD and cloud parameters have been previously observed, they are likely due to the swelling of aerosol particles in humid airmasses (Quaas et al, 2010), rather than an aerosol influence, which is in agreement with findings by, e.g., Myhre et al. (2007), Twohy et al. (2009) and Quaas et al. (2010).

#### 4.6.2 Interaction detector analysis

The  $q$  values of the combined effect of two parameters (AOD, RH, LTS, PVV) ~~interactive  $q$  statistic values for the influence of AOD and meteorological parameters on~~ the cloud parameters over the YRD and the ECS, derived using the GDM as described in Section 3.2, are ~~graphically~~ presented in the matrix shown in Figure 7-10, with the  $q$  values color coded. The data in Figure 7-10 show that the ~~interactive  $q$ -values for the interaction of a pair of factors~~ are larger than the  $q$ -values for any of the individual parameters (Table 45). Over the ECS, the combined ~~influences—effects~~ all exhibit a ~~binary nonlinear/bilinear~~ enhancement over the time period of this analysis. ~~Calculations show that~~ ~~the  $q$  values for the combined effects on CER over the ECS show that of AOD and RH on the CER results in the highest explanatory power of AOD together with each of the three meteorological parameters, RH, LTS and PVV is high with 92%, 86%, 84% and 94%, respectively as indicated by the  $q$  value (color bar at the bottom).~~ Also for the combination of LTS and PVV the explanatory power is high (90%). Further inspection of the data in Figure 7-10 shows that the explanatory powers of the combined effects are high for several combinations of parameters, such as ~~for CER combining AOD with LTS or PVV, and LTS with PVV,~~ for COT the combination of AOD with RH, LTS or PVV ~~or LTS with PVV, etc.~~ The data in Figure 7-10 show that the combination of AOD and ~~RH-PVV~~ results in high explanatory power for their influence on ~~all 54~~ cloud parameters (CER, COT, LWP and CF) and the combination of LTS with ~~PVV~~ RH has high explanatory power for their effects on ~~CER, COT, LWP and CTP.~~ Among the meteorological parameters, we find that the combined effect of AOD and PVV predominately influences ~~on~~ cloud

parameters over the ECS. The result is in accord with the findings of Jones et al. (2009) and Jia et al. (2022) that stronger aerosol cloud interactions typically occur under higher updraft velocity conditions.

Over the YRD, half of the ~~interactions~~ q values for the combined effects on cloud properties exhibit

835 nonlinear enhancement ~~of the influence of the independent parameters on the cloud properties~~ over the time period of this analysis, ~~infer~~ indicating that the combined effects on cloud properties are much

larger than that over the ECS. The data in Figure 7-10 show that the combination of AOD and RH results in high explanatory power for their influence on CER and COT, and the combination of AOD with LTS

has high explanatory power for their effects on LWP and CTP. The results in Figure 7-10 show that ~~the~~

840 combined effects of ~~AOD~~ PVV and LTS on the CF result in the highest explanatory power of ~~0.70~~ 0.84.

The data in Fig. 7-10 also show that the explanatory power is largest for the combined influence of AOD together with other factors, and is somewhat larger than the influence of AOD alone (Table 56) for all 5

cloud parameters. To some extent, this also applies to RH. What's more, the data do show that

meteorological factors enhance the explanatory power of the ~~cloud factors~~ AOD on cloud parameters over

845 ~~both two regions;~~ for ~~For~~ example, the individual q values for the influence of AOD and PVV over the

ECS were 0.83-81 and 0.69-0.70 but for the combined influence the q-statistic is as high as 0.9092. May

~~be we need to write more here~~ The results from the GDM interaction detector analysis clearly show the

enhancement of the interaction q-values over the q-values for the individual factors. In other words, the

explanatory power of the combined effects of aerosol and a meteorological parameter ~~and aerosol~~ is

850 larger than that of each parameter alone. Thus, the GDM provides an alternative way to obtain

information on confounding effects of different parameters. We can conclude that aerosol and

meteorological conditions do make a significant contribution to cloud parameters and that confounding

effects of different factors are often more important than each parameter alone and that the relative

importance of each parameter differs significantly over the ECS and YRD.

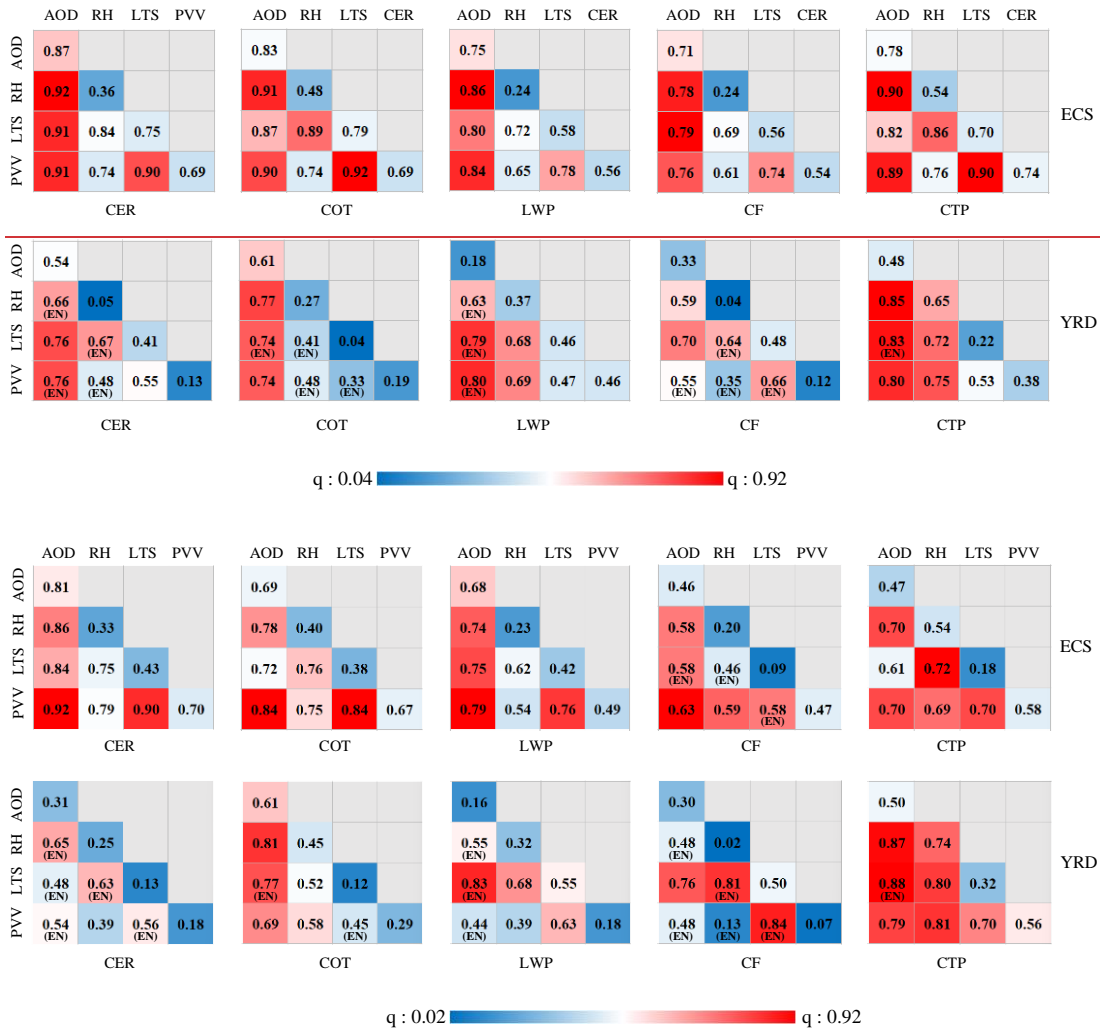


**Figure 710.** q values derived using the GDM for the combined effects of AOD, RH, LTS and PVV on cloud parameters Interactive-proxy variable q-statistics over the ECS (top) and the YRD (bottom). In addition to the numbers, the q values are colour coded according to the colour scale (linear from 0.04 to 0.92) at the bottom, for easy identification. –Note:– (EN) below a q value indicates the nonlinear enhancement of two variables (if  $q(x1 \cap x2) > q(x1) + q(x2)$ ), the absence of a and no-label below a q value denotes the indicates a binary-bilinear enhancing of two variables (if  $q(x1 \cap x2) > \text{Max}[q(x1), q(x2)]$ ) (Wang and Hu, 2012).

**5 Conclusions Discussion**

Warm cloud properties over eastern China have been investigated in relation to aerosol and meteorological conditions using 15 years (2008-2022) of data from passive (MODIS/Aqua) satellite measurements, together with the ECMWF ERA-5 reanalysis data ERA-Interim Reanalysis meteorological data. The Yangtze River Delta, a heavily polluted region in eastern China, and the East China Sea with a relatively clean atmosphere, were selected as study areas. Relationships between cloud droplet effective radius and AOD (used as a proxy for aerosol concentration CCN), i.e. characterized by the sensitivity S

870 ~~of CER to changes in AOD aerosol-cloud interaction (ACI) index~~, were constructed for different constraints of AOD and LWP. The effects of AOD on CER were investigated for three AOD regimes. In view of the uncertainty of MODIS-retrieved AOD and the scatter in the CER/AOD relations, data for AOD < 0.1 were not considered ~~in this study~~. In the moderately polluted AOD regime (0.1 < AOD < 0.3) ~~AOD regime, with 0.1 to 0.3~~, the CER over the YRD did not change significantly with AOD, whereas over the ECS the CER strongly decreased with AOD and the derived relationship between CER and AOD is statistically significant. In the third AOD regime, with AOD > 0.3, ~~over the YRD~~ the CER increased with increasing AOD over the YRD. In contrast, over the ECS there was no clear relation between CER and AOD, although CER variability increased with AOD > 0.3, especially for higher AOD (> ~0.8); ~~whereas over the ECS the CER did not significantly change as function of AOD, although the variations in the CER increased with AOD, especially for higher AOD (> ~0.8)~~. Based on these results, two different AOD regimes were selected for further investigation of ~~the ACI~~ aci: 0.1 < AOD < 0.3 over the ECS and AOD > 0.3 over the YRD. The spatial distribution of SACI, here defined as the relative change in CER as a function of the relative change in AOD (eq Eq. 1), averaged over the 15-years study period, shows that it was negative and statistically significant over the ECS and positive over the YRD. These results were obtained using data with no restriction on LWP. Stratification by Further selection of the data in different LWP intervals shows that over the YRD, for AOD greater than 0.3, ACI-S is negative positive for LWP in the interval [0-120 g m<sup>-2</sup>] with very small differences between three LWP intervals (0-40, 40-80 and 80-120 g m<sup>-2</sup>). In contrast, over the ECS, for AOD in the range from 0.1 to 0.3, ACI-S is positive-negative in the LWP interval [40-200 g m<sup>-2</sup>] and the value of S is re-are substantially differences different between the 4 LWP intervals, with ACI-S increasing with LWP, as shown in Table 23.–

885 These results were obtained using data from a period of 15 years. During this period, the aerosol properties changed in response to expanding economy, resulting in the increase of the AOD until 2007, and the implementation of emission reduction policy resulting in the decrease of the AOD from 2014 which flattened from about 2018 (de Leeuw et al., 2021; 2022; 2023). To account for these changes, the sensitivity S was determined for the periods 2008-2014 and 2014-2022, without stratification for LWP (see Figures xx FF: the 4 figures in the response in the Supplementary). The results for the ECS show no significant difference between the CER-AOD relations during these two periods. Over the YRD, however, the data for 2008-2014 show a clear decrease of CER with increasing AOD for 0.1 < AOD < 0.3

890

895



900 and for larger AOD the CER increased, with a statistical significant correlation ( $R=0.87$ ) and  $S=0.10$  as compared to  $S=0.08$  for the whole period. In contrast, the data for 2014-2022 show no clear correlation between CER and AOD for both AOD intervals over the YRD. A similar exercise for shorter periods, i.e. for each year between 2008 and 2022, show similar behavior as for the whole period 2008-2022, over both study areas, with interannual variations of the value of  $S$ . However, the statistical significance is low (large  $p$ ) due to the small number of data samples in each year.

905 It is noticed that in recent papers (e.g., Gryspeerdt et al., 2023; Arola et al., 2022) the usefulness of correlating aerosol and cloud parameters has been seriously challenged because cloud variability and retrieval errors are such that correlations between aerosol optical depth AOD and cloud properties ( $N_d$ , CER, LWP) can be spurious. Gryspeerdt et al. (2023) discussed  $ACI_{aci}$  in terms of the susceptibility  $\beta$  of  $N_d$  to aerosol rather than the sensitivity  $S$  of CER to aerosol (see the discussion in the Introduction on the use of  $N_d$  vs CER), and the problem arises with low aerosol conditions due to larger aerosol retrieval uncertainty due to surface correction (larger surface effect on the radiance at the top of the atmosphere), which applies equally to  $\beta$  and  $S$ . In the current study we did not consider the lowest aerosol conditions by limiting the data to situations with  $AOD \geq 0.1$ , as discussed in Section 4.2. Furthermore, we stratified the analysis for moderate ( $0.1 \leq AOD < 0.3$ ) and high ( $0.3 \leq AOD$ ) aerosol regimes, based on the data.

915 Arola et al. (2022) addressed the susceptibility of  $N_d$  to changes in aerosol and the adjustment of LWP (using satellite observations), and confounding factors, in particular co-variability of  $N_d$  and LWP induced by meteorological effects. They show how errors in the retrieved CER and COT or spatial heterogeneity in cloud fields influence the  $N_d$  - LWP relation. However, both  $N_d$  and LWP are not retrieved but derived from CER and COT. Using Eq. 1 and Eq. 2 in Arola et al. (2022), the  $N_d$ -LWP relationship can be shown to have a highly non-linear dependence on CER and thus it is no surprise that any error in CER strongly affects the relation between  $N_d$  and LWP. Their experiments, i.e. using smaller scales ( $5^\circ \times 5^\circ$ ) to reduce spatial meteorological variability, or using snapshots to remove meteorological variability in time, did not lead to a conclusion whether the  $N_d$  - LWP variability is due to spatial heterogeneity in the cloud fields or due to retrieval errors. The main message from this part of the study (using satellite data) by Arola et al. (2022) is “the spatial variability of CER introduces a bias which moreover becomes stronger in conditions where the CER values are lower on average”.

920

925

Experiments with simulated measurements show that “the main cause of the negative LWP vs  $N_d$  slopes is the error in CER”. Arola et al. emphasize that the spatial cloud variability and retrieval errors in CER and COT are similar sources for negative bias in LWP adjustment and that these sources could not be separately assessed in their simulations. The implication of the findings of Arola et al. (2022) on the adjustment of LWP for the results of the current study on the sensitivity of CER to aerosol (or CCN, using AOD as proxy) is that the assumption of constant LWP may be violated. This would affect the results presented in Section 4.3 where LWP was stratified and S was found to vary with LWP. In view of the LWP adjustment to changes in aerosol, the variation of CER sensitivity with LWP may be somewhat different from that reported in section 4.3.

The above results were obtained by using traditional statistical methods where relationships were derived from scatterplots of CER versus AOD, stratified in two different AOD regimes and five different LWP regimes, as discussed above. The data were also analyzed by ~~By~~ using the ~~geographical detector method~~ GDM to determine which factors influence ~~ACI~~aci and identify how interactions between different parameters influence the results of the aci analysis, i.e. the sensitivity and resulting adjustments. In particular, the GDM provides information on the extent to which the effect of individual factors is influenced by other factors. As shown in Section 4.6.1, the effect of individual factors may be overestimated when confounding effects of other factors are not accounted for. The interaction detector analysis (Section 4.26.2) shows a more realistic estimate of the effects on aci when different factors are analyzed together. The factor detector analysis (Section 4.6.1) shows that ~~the influence of different parameters (AOD and meteorological parameters) on the cloud properties in eastern China has been investigated.~~ Over the ECS, AOD has the largest influence on cloud parameters, as indicated by the large and statistically significant q values. Among the meteorological factors, ~~LTS~~ PVV has more influence on the variations of the cloud parameters than RH and ~~PVV~~LTS. Over the YRD, AOD has the largest influence on ~~CER and~~ COT, with large and significant q values. Among the meteorological factors, the effect of LTS on CF is greater than that of RH and PVV. However, ~~the~~ the q-values may sum up to over 100% when the variables are not independent, i.e. the explanatory power of such variables is too high. The evaluation of the effects of interaction between different factors on aci corrects these clearly unrealistic situations. The analysis in section 4.26.2 shows that the interactive q-statistic values derived in this study ~~were~~ are larger than any of the values for single variables, i.e. the explanatory power of a

combination of factors is higher than that of individual factors, but less than 100%. The combined influences of AOD and meteorological parameters exhibit binary nonlinear enhancement of the explanatory power of the variation of the cloud parameters. However, although the GDM ~~this work can therefore only~~ provides further evidence of the effects of aerosol and meteorological factors and their interactions ~~effect~~ on cloud properties and quantify the relative contributions ~~and combined effects on clouds to aci~~, it ~~but~~ cannot quantify the absolute contributions with confidence.

## 6 Conclusions

The response of different cloud parameters to variations in AOD and in meteorological conditions has been analyzed using traditional statistical methods to determine the sensitivity  $S$  of CER to aerosol for different aerosol regimes and stratified according to LWP. The results show the contrasting behavior over a polluted region over land (YRD) and a relatively clean region over ocean (ECS). In the intermediate aerosol regime ( $0.1 < \text{AOD} < 0.3$ ), CER does not significantly change with AOD over the YRD ( $S \approx 0$ ), but over the ECS  $S$  is negative and increases with increasing LWP. In the high aerosol regime ( $\text{AOD} > 0.3$ ),  $S$  is positive over the YRD but varies little with LWP, whereas over the ECS the CER does not change with AOD. These results may be influenced by confounding effects of meteorological parameters. The study further shows that over the ECS the CER is larger for higher LTS and RH but lower for higher PVV. Over the YRD, there is no significant influence of LTS on the relationship between CER and AOD.

The GDM has been applied to determine which factors influence  $S$  and cloud parameters and the interaction detector analysis has been used to determine the combined effect of different parameters on cloud parameters. ~~The results show that o~~Over the ECS, with the increase of the AOD, the CER and CTP decrease, and the COT and CF increase. Over the YRD, with the increase of the AOD, the CER and CTP increase, and the COT and cloud cover decrease. The CER is larger in unstable atmospheric conditions than in stable conditions, irrespective of the AOD. The cloud fraction is much larger in high relative humidity RH conditions than in low relative humidity RH conditions. However, the impact of vertical velocity PVV on the CER is weak in polluted and heavily polluted conditions. In general, the influence of the AOD on the CER is greater than that of meteorological conditions. Therefore, AOD plays a dominant role in the effects of different factors on CER.

The results from the GDM interaction detector analysis clearly show the enhancement of the interaction

985 q-values over the q-values for the individual factors. In other words, the explanatory power of the  
combined effects of aerosol and a meteorological parameter is larger than that of each parameter alone.  
Thus, the GDM provides an alternative way to obtain information on confounding effects of different  
parameters. We conclude that aerosol and meteorological conditions significantly influence cloud  
parameters and that combined effects of different factors are often more important than the effect of each  
990 individual factor. The relative importance of each factor differs significantly over the ECS and  
YRD. Different from previous studies, here the interaction between aerosol and CER has been  
investigated by considering different AOD and LWP regimes on ACI over land and ocean. The relative  
importance of AOD and meteorological parameters on cloud properties were examined by using the  
geographical detector method.

995 The results of this study contribute to improve the understanding of the indirect effects of aerosols and  
the role of various driving factors on the cloud microphysical properties. By comparing son with aerosol  
and cloud observational data of aerosols and clouds, the regional climate model's ability to simulate  
changes in cloud parameters can be evaluated. A more accurate description of the relative contribution  
of meteorological factors can improve the parameterization scheme of the model over eastern China.  
1000 They  
provide a reference for improving the parameterization scheme of regional climate models in eastern  
China.

#### ***Data availability***

All data used in this study are publicly available. The satellite data from the MODIS instrument used in  
this study were obtained from <https://ladsweb.nascom.nasa.gov/search/> (last access: 12 July 2022, Liu,  
1005 2022a). The the ECMWF ERA-5 reanalysis data were collected from the ECMWF ERA-5 reanalysis  
data server [https://cds.climate.copernicus.eu/cdsapp#!/dataset/reanalysis-era5-pressure-levels-monthly-](https://cds.climate.copernicus.eu/cdsapp#!/dataset/reanalysis-era5-pressure-levels-monthly-means?tab=form)  
[means?tab=form](https://cds.climate.copernicus.eu/cdsapp#!/dataset/reanalysis-era5-pressure-levels-monthly-means?tab=form) (last access: 12 July 2022, Liu, 2022b).

#### ***Author contributions***

YL and GL designed the research. YL led the analyses. YL and LT wrote the manuscript with major  
1010 input from JH, GL and further input from all other authors. All authors contributed to interpreting the  
results and to the finalization and revision of the manuscript.

### *Competing interests*

The authors declare that they have no conflict of interest.

### *Acknowledgements*

1015 This work was supported by the National Natural Science Foundation of China (Grant No. 42001290),  
and the Natural Science Foundation of China (Grant No. 41871253). We are grateful for the easy access  
to MODIS data products provided by NASA. We also thank ECMWF for providing daily ERA-5 [Interim](#)  
reanalysis data. The study contributes to the ESA / MOST cooperation project DRAGON5, Topic 3  
Atmosphere, sub-topic 3.2 Air-Quality.

### 1020 **References**

- [Ahn, E., Huang, Y., Siems, S. T., & Manton, M. J.: A comparison of cloud microphysical properties derived from MODIS and CALIPSO with in situ measurements over the wintertime Southern Ocean. \*Journal of Geophysical Research: Atmospheres\*, 123, 11,120–11,140. <https://doi.org/10.1029/2018JD028535>, 2018.](#)
- 1025 [Andersen, H., & Cermak, J.: How thermodynamic environments control stratocumulus microphysics and interactions with aerosols. \*Environmental Research Letters\*, 10, 024004. <https://doi.org/10.1088/1748-9326/10/2/024004>, 2015.](#)
- [Arola, A., Lipponen, A., Kolmonen, P., Virtanen, T.H., Bellouin, N., Grosvenor, D. P., Gryspeerdt, E., Quaas, J., and Kokkola, H., Aerosol effects on clouds are concealed by natural cloud heterogeneity and satellite retrieval errors, \*Nature Communications\*, 13:7357 \(8 pp.\), <https://doi.org/10.1038/s41467-022-34948-5>, 2022.](#)
- 1030 [Andreae, M. O.: Correlation between cloud condensation nuclei concentration and aerosol optical thickness in remote and polluted regions, \*Atmos. Chem. Phys.\*, 9, 543-556, <https://doi.org/10.5194/acp-9-543-2009>, 2009.](#)
- 1035 [Albrecht, B. A.: Aerosols, cloud microphysics, and fractional cloudiness, \*Science\*, 245, 1227-1230, 1989.](#)  
[Bellouin, N., Quaas, J., Gryspeerdt, E., Kinne, S., Stier, P., Watson-Parris, D., et al.: Bounding global aerosol radiative forcing of climate change. \*Reviews of Geophysics\*, 58, e2019RG000660. <https://doi.org/10.1029/2019RG000660>, 2020.](#)

- 1040 Brewer C. A., Pickle L.: Evaluation of methods for classifying epidemiological data on choropleth maps in series. *Annals of the Association of American Geographers*, 92(4), 662–81, 2002.
- [Boucher, O., Quaas, J.: Water vapour affects both rain and aerosol optical depth. \*Nature Geoscience\*, 6\(1\), 4–5. <https://doi.org/10.1038/ngeo1692>, 2012.](#)
- Burrows, J. P., Platt, U., Borrell, P.: The remote sensing of tropospheric composition from space, Springer Verlag, Heidelberg, Germany, 2011.
- 1045 [Che, H. Z., Yang, L.K., Liu, C., Xia, X. A., Wang, Y. Q., Wang, H., Wang, H., Lu, X. F., Zhang, X. Y., Huizheng Che, Leiku Yang, Chao Liu, Xiangao Xia, Yaqiang Wang, Hong Wang, Han Wang, Xiaofeng Lu, Xiaoye Zhang, Long-term validation of MODIS C6 and C6.1 Dark Target aerosol products over China using CARSNET and AERONET. \*Chemosphere\*, Volume 236, 2019, 124268, ISSN 0045-6535, <https://doi.org/10.1016/j.chemosphere.2019.06.238>, 2019.](#)
- 1050 Christensen, M. W., Jones, W. K., Stier, P.: Aerosols enhance cloud lifetime and brightness along the stratus-to-cumulus transition, *Proceedings of the National Academy of Sciences*, 117(30), 17591-17598.
- Chen, Y.-C., Christensen, M. W., Stephens, G. L., and Seinfeld, J. H.: Satellite-based estimate of global aerosol-cloud radiative forcing by marine warm clouds, *Nat. Geosci.*, 7, 643–646, <https://doi.org/10.1038/ngeo2214>, 2014.
- 1055 Christensen, M. W., Chen, Y.-C., and Stephens, G. L.: Aerosol indirect effect dictated by liquid clouds, *J. Geophys. Res.*, 121, 14636–14650, <https://doi.org/10.1002/2016JD025245>, 2016.
- Costantino, L. and Bréon, F. M.: Analysis of aerosol-cloud interaction from multi-sensor satellite observations. *Geophys. Res. Lett.*, 37, L11801, doi:10.1029/2009GL041828, 2010.
- Costantino, L. and Bréon, F. M.: Aerosol indirect effect on warm clouds over South-East Atlantic, from 1060 co-located MODIS and CALIPSO observations, *Atmos. Chem. Phys.*, 13: 69-88, 2013.
- de Leeuw, G., Andreas, E. L., Anguelova, M. D., Fairall, C. W., Lewis, E. R., O'Dowd, C., Schulz, M., and Schwartz, S. E. Schwartz.: Production flux of sea spray aerosol, *Rev. Geophys.*, 49, RG2001, doi:10.1029/2010RG000349, 2011.
- de Leeuw, G., Sogacheva, L., Rodriguez, E., Kourtidis, K., Georgoulas, A. K., Alexandri, G., Amiridis, 1065 V., Proestakis, E., Marinou, E., Xue, Y., and van der A, R.: Two decades of satellite observations of AOD over mainland China using ATSR-2, AATSR and MODIS/Terra: data set evaluation and large-scale patterns, *Atmos. Chem. Phys.*, 18, 1573-1592, <https://doi.org/10.5194/acp-18-1573-2018>, 2018.

Fan J, Wang Y, Rosenfeld D, et al.: Review of aerosol-cloud interactions: Mechanisms, significance, and challenges. *Journal of the Atmospheric Sciences*,73(11): 4221-4252, 2016.

1070 [de Leeuw, G., R. van der A, J. Bai, Y. Xue, C. Varotsos, Z. Li, C. Fan, X. Chen, I. Christodoulakis, J. Ding, X. Hou, G. Kouremadas, D. Li, J. Wang, M. Zara, K. Zhang, Y. Zhang-\(2021\): Air Quality over China. \*Remote Sens.\* 2021, 13, 3542. <https://doi.org/10.3390/rs13173542>, 2021.](#)

de Leeuw, G., Fan, C, Li, Z., Dong, J., Li, Y., Ou, Y., and Zhu, S. (2022). Spatiotemporal variation and provincial scale differences of the AOD across China during 2000–2021. *Atmospheric Pollution Research* 13 (2022) 101359 (14 pp). <https://doi.org/10.1016/j.apr.2022.101359>.

1075 de Leeuw, G., Kang, H., Fan, C., Li, Z., Fang, C., Zhang, Y. (2023). Meteorological and anthropogenic contributions to changes in the Aerosol Optical Depth (AOD) over China during the last decade. *Atm. Env.*, 301, 119676. <https://doi.org/10.1016/j.atmosenv.2023.119676>.

Feingold, G., Remer, L. A., Ramaprasad, J., Kaufman, Y. J.: Analysis of smoke impact on clouds in Brazilian biomass burning regions: an extension of Twomey’s approach, *J. Geophys. Res.*, 106 (D19), 22907-22922, 2001.

1080 [Fu, D., Di Girolamo, L., Rauber, R. M., McFarquhar, G. M., Nesbitt, S. W., Loveridge, J., Hong, Y., van Diedenhoven, B., Cairns, B., Alexandrov, M. D., Lawson, P., Woods, S., Tanelli, S., Schmidt, S., Hostetler, C., and Scarino, A. J.: An evaluation of the liquid cloud droplet effective radius derived from MODIS, airborne remote sensing, and in situ measurements from CAMP2Ex, \*Atmos. Chem. Phys.\*, 22, 8259–8285. <https://doi.org/10.5194/acp-22-8259-2022>, 2022.](#)

Grandey, B.S., Stier, P.: A critical look at spatial scale choices in satellite-based aerosol indirect effect studies. *Atmos. Chem. Phys.*, 10, 11459-11470, 2010.

1090 Gryspeerdt, E., Stier, P., and Partridge, D. G.: Satellite observations of cloud regime development: the role of aerosol processes, *Atmos. Chem. Phys.*, 14, 1141-1158, doi:10.5194/acp-14-1141-2014, 2014.

[Gryspeerdt, E., Povey, A. C., Grainger, R. G., Hasekamp, O., Hsu, N. C., Mulcahy, J. P., Sayer, A. M., and Sorooshian, A.: Uncertainty in aerosol–cloud radiative forcing is driven by clean conditions, \*Atmos. Chem. Phys.\*, 23, 4115–4122. <https://doi.org/10.5194/acp-23-4115-2023>, 2023.](#)

1095 [Gryspeerdt, E., Stier, P., & Grandey, B. S.: Cloud fraction mediates the aerosol optical depth-cloud top height relationship. \*Geophysical Research Letters\*, 41, 3622-3627. <https://doi.org/10.1002/2014GL059524>, 2014.](#)

[Gryspeerd, Edward, Quaas, J., Ferrachat, S., Gettelman, A., Ghan, S., Lohmann, U., et al.: Constraining the instantaneous aerosol influence on cloud albedo. Proceedings of the National Academy of Sciences of the United States of America, 114\(19\), 4899-4904. <https://doi.org/10.1073/pnas.1617765114>, 2017.](#)

1100 Huang, H., Thomas, G. E., and Grainger, R. G.: Relationship between wind speed and aerosol optical depth over remote ocean, *Atmos. Chem. Phys.*, 10, 5943-5950, <https://doi.org/10.5194/acp-10-5943-2010>, 2010.

Jia, H. L., Ma, X. Y., Quaas, J., Yin, Y., Qiu, T.: Is positive correlation between cloud droplet effective radius and aerosol optical depth over land due to retrieval artifacts or real physical processes? *Atmospheric Chemistry and Physics*, 19, 13, 8879-8896, 2019.

1105 [Jia, H., Quaas, J., Gryspeerd, E., Böhm, C., & Sourdeval, O.-\(2022\): Addressing the difficulties in quantifying droplet number response to aerosol from satellite observations. \*Atmospheric Chemistry and Physics\*, 22\(11\), 7353–7372. <https://doi.org/10.5194/acp-22-7353-2022>, 2022.](#)

Jin, M. L. and Shepherd, J. M.: Aerosol relationships to warm season clouds and rainfall at monthly scales over east China: Urban land versus ocean, *J. Geophys. Res.*, 113, D24S90, <https://doi.org/10.1029/2008JD010276>, 2008.

[Jones, T. A., Christopher, S. A., & Quaas, J.: A six year satellite-based assessment of the regional variations in aerosol indirect effects. \*Atmospheric Chemistry and Physics\*, 9, 4091, 2009.](#)

1115 Kaufman, Y.J. and Fraser, R.S.: The effect of smoke particles on clouds and climate forcing. *Science*, 1997. 277(5332): p. 1636-1639.

Klein, S. A. and Hartmann, D. L.: The seasonal cycle of low stratiform clouds, *J. Climate*, 6, 1587-1606, 1993.

Koren, I., Kaufman, Y. J., Rosenfeld, D., Remer, L. A., Rudich, Y.: Aerosol invigoration and restructuring of Atlantic convective clouds. *Geophys. Res. Lett.*, 32 (14), L14828, 2005.

1120 Koren, I., Martins, J. V., Remer, L. A., and Afargan, H.: Smoke invigoration versus inhabitation of clouds over the Amazon, *Science*, 321, 946-949, doi:10.1126/science.1159185, 2008.

[Koren, I., Feingold, G., & Remer, L. A.: The invigoration of deep convective clouds over the Atlantic: aerosol effect, meteorology or retrieval artifact? \*Atmospheric Chemistry and Physics\*, 10\(18\), 8855–8872. <https://doi.org/10.5194/acp-10-8855-2010>, 2010.](#)



- 1125 Kourtidis, K., Stathopoulos, S., Georgoulas, A. K., Alexandri, G., and Rapsomanikis, S.: A study of the impact of synoptic weather conditions and water vapor on aerosol-cloud relationships over major urban clusters of China, *Atmos. Chem. Phys.*, 15, 10955-10964, doi:10.5194/acp-15-10955-2015, 2015.
- Levy, R. C., Mattoo, S., Munchak, L. A., Remer, L. A., Sayer, A. M., Patadia, F., and Hsu, N. C.: The Collection 6 MODIS aerosol products over land and ocean, *Atmos. Meas. Tech.*, 6, 2989-3034, 1130 <https://doi.org/10.5194/amt-6-2989-2013>, 2013.
- Li, Z. Q., Guo, J. P., Ding, A. J., Liao, H., Liu, J. J., Sun, Y. L., Wang, T. J., Xue, H. W., Zhang, H. S., Zhu, B.: Aerosol and boundary-layer interactions and impact on air quality. *National Science Review* 4: 810-833, 2017, doi: 10.1093/nsr/nwx117, 2017.
- Liu, Y. Q.: MODIS L3 collection 6.1 data, Institute of Urban Environment, Chinese Academy of 1135 Sciences, available at: <https://ladsweb.nascom.nasa.gov/search/>, last access: 12 July 2022a.
- Liu, Y. Q.: ECMWF ERA-5 reanalysis data set, Institute of Urban Environment, Chinese Academy of Sciences, available at: <https://cds.climate.copernicus.eu/cdsapp#!/dataset/reanalysis-era5-pressure-levels-monthly-means?tab=form>, last access: 12 July 2022b.
- Liu, Y., de Leeuw, G., Kerminen, V.-M., Zhang, J., Zhou, P., Nie, W., Qi, X., Hong, J., Wang, Y., Ding, 1140 A., Guo, H., Krüger, O., Kulmala, M., and Petäjä, T.: Analysis of aerosol effects on warm clouds over the Yangtze River Delta from multi-sensor satellite observations, *Atmos. Chem. Phys.*, 17, 5623–5641, <https://doi.org/10.5194/acp-17-5623-2017>, 2017.
- Liu, Q., Duan, S. Y., He, Q. S., Chen, Y. H., Zhang, H., Cheng, N. X., Huang, Y. W., Chen, B., Zhan, Q. Y., Li, J. Z.: The variability of warm cloud droplet radius induced by aerosols and water vapor in 1145 Shanghai from MODIS observations, *Atmospheric Research*, 253, 105470, 2021.
- Liu, T. Q., Liu, Q., Chen, Y. H., Wang, W. C., Zhang, H., Li, D., Sheng, J.: Effect of aerosols on the macro- and micro-physical properties of warm clouds in the Beijing-Tianjin-Heibei region. *Science of the Total Environment*, 720, 137618, 2020.
- Liu, Y., Zhang, J., Zhou, P., Lin, T., Hong, J., Shi, L., Yao, F., Wu, J., Guo, H., and de Leeuw, G.: 1150 Satellite-based estimate of the variability of warm cloud properties associated with aerosol and meteorological conditions, *Atmos. Chem. Phys.*, 18, 18187-18202, <https://doi.org/10.5194/acp-18-18187-2018>, 2018.

1155 Liu, Y., de Leeuw, G., Kerminen, V.-M., Zhang, J., Zhou, P., Nie, W., Qi, X., Hong, J., Wang, Y., Ding, A., Guo, H., Krüger, O., Kulmala, M., and Petäjä, T.: Analysis of aerosol effects on warm clouds over the Yangtze River Delta from multi-sensor satellite observations, *Atmos. Chem. Phys.*, 17, 5623-5641, <https://doi.org/10.5194/acp-17-5623-2017>, 2017.

1160 Liu, Y., Lin, T., Hong, J., Wang, Y., Shi, L., Huang, Y., Wu, X., Zhou, H., Zhang, J., and de Leeuw, G. (2021). Multi-dimensional satellite observations of aerosol properties and aerosol types over three major urban clusters in eastern China, *Atmos. Chem. Phys.*, 21, 12331–12358, <https://doi.org/10.5194/acp-21-12331-2021>, 2021.

Lohmann, U., Rotstajn, L., Storelvmo, T., Jones, A., Menon, S., Quaas, J., Ekman, A.M.L., Koch, D., Ruedy, R.: Total aerosol effect: radiative forcing or radiative flux perturbation? *Atmospheric Chemistry and Physics*, 10 (7): p. 3235-3246, 2010.

1165 [Ma, X., Jia, H., Yu, F., & Quaas, J. \(2018\): Opposite aerosol index-cloud droplet effective radius correlations over major industrial regions and their adjacent oceans. \*Geophysical Research Letters\*, 45, 5771–5778. <https://doi.org/10.1029/2018GL077562>, 2018.](#)

Matheson, M. A., Coakley Jr., J. A., and Tahnk, W. R.: Aerosol and cloud property from relationships for summer stratiform clouds in the northeastern Atlantic from advanced very high resolution radiometer observations, *J. Geophys. Res.*, 110, D24204, doi:10.1029/2005JD006165, 2005.

1170 [McComiskey, A., & Feingold, G. \(2012\): The scale problem in quantifying aerosol indirect effects. \*Atmospheric Chemistry and Physics\*, 12, 1031. <https://doi.org/10.5194/acp-12-1031-2012>, 2012.](#)

Meskhidze, N., Nenes, A.: Effects of ocean ecosystem on marine aerosol-cloud interaction. *Adv. Meteorol*, doi:10.1155/2010/239808, 2010.

1175 Michibata, T., Kawamoto, K., and Takemura, T.: The effects of aerosols on water cloud microphysics and macrophysics based on satellite-retrieved data over East Asia and the North Pacific, *Atmos. Chem. Phys.*, 14, 11935-11948, <https://doi.org/10.5194/acp-14-11935-2014>, 2014.

[Myhre, G., Stordal, F., Johnsrud, M., Kaufman, Y. J., Rosenfeld, D., Storelvmo, T., et al.: Aerosol-cloud interaction inferred from MODIS satellite data and global aerosol models. \*Atmospheric Chemistry and Physics\*, 7\(12\), 3081–3101. <https://doi.org/10.5194/acp-7-3081-2007>, 2007.](#)

1180 [Nakajima, T., Higurashi, A., Kawamoto, K., and Penner, J. E.: A possible correlation between satellite-derived cloud and aerosol microphysical parameters, \*Geophys. Res. Lett.\*, 28, 1171–1174, <https://doi.org/10.1029/2000GL012186>, 2001.](#)

[Painemal, D., and Zuidema, P.: ~~Zuidema \(2011\)~~, Assessment of MODIS cloud effective radius and optical thickness retrievals over the Southeast Pacific with VOCALS-REx in situ measurements, \*J. Geophys. Res.\*, 116, D24206, doi:10.1029/2011JD016155, 2011.](#)

1185 Pandey, S. K., Vinoj, V., Panwar, A.: The short-term variability of aerosols and their impact on cloud properties and radiative effect over the Indo-Gangetic Plain. *Atmospheric Pollution Research*, 11, 630–638, 2020.

[Platnick, S., Meyer, K. G., King, M. D., Wind, G., Amarasinghe, N., Marchant, B., Arnold, G. T., Zhang, Z., Hubanks, P. A., Holz, R. E., Yang, P., Ridgway, W. L., Riedi, J.: The MODIS cloud optical and microphysical products: Collection 6 updates and examples from Terra and Aqua. \*IEEE Trans Geosci Remote Sens.\* 2017-Jan;55\(1\):502-525. doi: 10.1109/TGRS.2016.2610522, 2017.](#)

1190 [Qiu, Y, Zhao, C., Guo, J., Li, J.: 8-Year ground-based observational analysis about the seasonal variation of the aerosol-cloud droplet effective radius relationship at SGP site. \*Atmospheric Environment\* 164 139–146, 2017. <http://dx.doi.org/10.1016/j.atmosenv.2017.06.002>.](#)

1195 [Quaas, J., Boucher, O., Bellouin, N., Kinne, S.: Satellite-based estimate of the direct and indirect aerosol climate forcing, \*J. Geophys. Res.\*, 113, D05204, doi:10.1029/2007JD008962, 2008.](#)

[Quaas, J., Stevens, B., Stier, P., and Lohmann, U.: Interpreting the cloud cover – aerosol optical depth relationship found in satellite data using a general circulation model, \*Atmos. Chem. Phys.\*, 10, 6129–6135, <https://doi.org/10.5194/acp-10-6129-2010>, 2010.](#)

1200 [Rao, S., Dey, S.: Consistent signal of aerosol indirect and semi-direct effect on water clouds in the oceanic regions adjacent to the Indian subcontinent. \*Atmospheric Research\*, 232, 2020.](#)

[Remer, L. A., Kaufman, Y. J., Tanre, D., Mattoo, S., Chu, D. A., Martins, J. V., Li, R. R., Ichoku, C., Levy, R. C., Kleidman, R. G., Eck, T. F., Vermote, E., and Holben, B. N.: The MODIS aerosol algorithm, products, and validation, \*J. Atmos. Sci.\*, 62, 947–973, <https://doi.org/10.1175/JAS3385.1>, 2005.](#)

1205 [Rosenfeld, D. and Lensky, I. M.: Satellite-based insights into precipitation formation processes in continental and maritime convective clouds, \*B. Am. Meteorol. Soc.\*, 79, 2457–2476, 1998.](#)

1210 Rosenfeld, D., Andreae, M. O., Asmi, A., Chin, M., de Leeuw, G., Donovan, D., Kahn, R., Kinne, S.,  
Kivekäs, N., Kulmala, M., Lau, W., Schmidt, S., Suni, T., Wagner, T., Wild, M., and Quaas, J.: Global  
observations of aerosol-cloudprecipitation- climate interactions, *Rev. Geophys.*, 52, 750-808,  
doi:10.1002/2013RG000441, 2014.

Rosenfeld, D., Zhu, Y. N., Wang, M. H., Zheng, Y. T., Goren, T., Yu, S. C.: Aerosol-driven droplet  
concentrations dominate coverage and water of oceanic low-level clouds, *Science*, 363, 6427, 2019.

1215 Saponaro, G., Kolmonen, P., Sogacheva, L., Rodriguez, E., Virtanen, T., de Leeus, G.: Estimates of the  
aerosol indirect effect over the Baltic Sea region derived from 12 years of MODIS observations, *Atmos.*  
*Chem. Phys.*, 17, 3133-3143, 2017.

Sayer, A. M., Munchak, L. A., Hsu, N. C., Levy, R. C., Bettenhausen, C., and Jeong, M. J.: MODIS  
Collection 6 aerosol products: Comparison between Aqua’s e-Deep Blue, Dark Target, and “merged”  
data sets, and usage recommendations, *J. Geophys. Res.-Atmos.*, 119, 13965-13989,  
1220 <https://doi.org/10.1002/2014jd022453>, 2014.

[Sayer, A. M., Hsu, N. C., Bettenhausen, C., Jeong, M., Meister, G., and Al, S. E. T.: Effect of MODIS  
Terra radiometric calibration improvements on Collection 6 Deep Blue aerosol products: validation and  
Terra/Aqua consistency, \*J. Geophys. Res.-Atmos.\*, 120, 12157–12174,  
<https://doi.org/10.1002/2015JD023878>, 2015.](#)

1225 [Sayer, A. M.: Interactive comment on “Two decades of satellite observations of AOD over mainland  
China” by Gerrit de Leeuw et al., <https://doi.org/10.5194/acp-2017-838-RC1>, 2017.](#)

Seinfeld, J.H.; Pandis, S.N. *Atmospheric Chemistry and Physics: From Air Pollution to Climate Change*;  
John Wiley and Sons, Inc.: New York, 1998; ISBN 0-471-17815-2.

1230 Shen, L. J., Wang, H. L., Kong, X. C., Zhang, C., Shi, S. S., Zhu, B.: Characterization of black carbon  
aerosol in the Yangtze River Delta, China Seasonal variation and source apportionment, *Atmospheric  
Pollution Research*, 12, 195-209, 2021.

Shao, H. F and Liu, G. S.: Why is the satellite observed aerosol’s indirect effect so variable?, *Geophysical  
research letters*, 32, L15802, doi:10.1029/2005GL023260, 2005.

1235 Slingo, A.: Sensitivity of the Earth’s radiation budget to changes in low clouds, *Nature*, 343(6253), 49-  
51, 1990.

- Smirnov, A., Sayer, A. M., Holben, B. N., Hsu, N. C., Sakerin, S. M., Macke, A., Nelson, N. B., Courcoux, Y., Smyth, T. J., Croot, P., Quinn, P. K., Sciare, J., Gulev, S. K., Piketh, S., Losno, R., Kinne, S., and Radionov, V. F.: Effect of wind speed on aerosol optical depth over remote oceans, based on data from the Maritime Aerosol Network, *Atmos. Meas. Tech.*, 5, 377–388, <https://doi.org/10.5194/amt-5-377-2012>, 2012.
- 1240
- Sogacheva, L., Popp, T., Sayer, A. M., Dubovik, O., Garay, M. J., Heckel, A., Hsu, N. C., Jethva, H., Kahn, R. A., Kolmonen, P., Kosmale, M., de Leeuw, G., Levy, R. C., Litvinov, P., Lyapustin, A., North, P., Torres, O., and Arola, A.: Merging regional and global aerosol optical depth records from major available satellite products, *Atmos. Chem. Phys.*, 20, 2031–2056, <https://doi.org/10.5194/acp-20-2031-2020>, 2020.
- 1245
- [Su, W., Loeb, N. G., Xu, K. M., Schuster, G. L., and Eitzen, Z. A.: An estimate of aerosol indirect effect from satellite measurements with concurrent meteorological analysis, \*J. Geophys. Res.-Atmos.\*, 115, D18219, doi:10.1029/2010JD013948, 2010.](#)
- [Tan, S., Han, Z., Wang, B., & Shi, G.: Variability in the correlation between satellite-derived liquid cloud droplet effective radius and aerosol index over the northern Pacific Ocean. \*Tellus B: Chemical and Physical Meteorology\*, 69\(1\), 1391656. <https://doi.org/10.1080/16000889.2017.1391656>, 2017.](#)
- 1250
- [Tang, J., Wang, P., Mickley, L. J., Xia, X., Liao, H., Yue, X., et al.: Positive relationship between liquid cloud droplet effective radius and aerosol optical depth over Eastern China from satellite data. \*Atmospheric Environment\*, 84, 244–253. <https://doi.org/10.1016/j.atmosenv.2013.08.024>, 2014.](#)
- 1255
- Tao, W. K., Chen, J. P., Li, Z., Wang, C. E., Zhang, C. D.: Impact of aerosols on convective clouds and precipitation, *Reviews of Geophysics*, 50(2), 2012.
- Ten Hoeve, J. E., Remer, L. A., and Jacobson, M. Z.: Microphysical and radiative effects of aerosols on warm clouds during the Amazon biomass burning season as observed by MODIS: impacts of water vapor and land cover, *Atmos. Chem. Phys.*, 11, 3021–3036, doi:10.5194/acp-11-3021-2011, 2011.
- 1260
- [Twohy, C. H., Coakley Jr., J. A., and Tahnk, W. R.: Effect of changes in relative humidity on aerosol scattering near clouds. \*J. Geophys. Res.\*, 114, D05205, doi:10.1029/2008JD010991, 2009.](#)
- Twomey, S.: The influence of pollution on the shortwave albedo of clouds, *J. Atmos. Sci.* 34(7), 1149–1152, 1977.

- 1265 Wang, J. F., Li, X. H., Christakos, G., Liao, Y. L., Zhang, T., Gu, X., Zheng, X. Y.: Geographical detectors-based health risk assessment and its application in the neural tube defects study of the Heshun Region, China. *Int. J. Geogr. Inf. Sci.* 24, 107-127, 2010.
- Wang, J. F., Hu, Y.: Environmental health risk detection with GeogDetector. *Environ. Model. Softw.* 33, 114-115, 2012.
- 1270 Wang, J. F., Zhang, T. L., Fu, B. J.: A measure of spatial stratified heterogeneity. *Ecol. Indic.* 67, 250-256, 2016.
- Wang, J. X., Hu, M. G., Zhang, F. S., Gao, B. B.: Influential factors detection for surface water quality with geographical detectors in China. *Stoch. Environ. Res. Risk A* 32, 2633-2645, 2018.
- 1275 Wang, F., Guo, J., Zhang, J., Huang, J., Min, M., Chen, T., Liu, H., Deng, M., Li, X.: Multi-sensor quantification of aerosol-induced variability in warm clouds over eastern China, *Atmos. Environ.*, 113: 1-9, 2015. <http://dx.doi.org/10.1016/j.atmosenv.2015.04.063>.
- [Wei, J., Li, Z., Peng, Y., Sun, L.: MODIS Collection 6.1 aerosol optical depth products over land and ocean: validation and comparison, Atmospheric Environment, Volume 201, 2019, Pages 428-440, ISSN 1352-2310, https://doi.org/10.1016/j.atmosenv.2018.12.004, 2019.](https://doi.org/10.1016/j.atmosenv.2018.12.004)
- 1280 Wood, R. and Bretherton, C. S.: On the relationship between Stratiform Low Cloud Cover and Lower-Tropospheric Stability, *J. Climate*, 19, 6425-6432, 2006.
- [Yuan, T., Li, Z., Zhang, R., and Fan, J.: Increase of cloud droplet size with aerosol optical depth: an observation and modeling study, J. Geophys. Res., 113, D04201, doi:10.1029/2007JD008632, 2008.](https://doi.org/10.1029/2007JD008632)
- 1285 Zhao, C. F., Qiu, Y. M., Dong, X. B., Wang, Z. E., Peng, Y. R., Li, B. D., Wu, Z. H., Wang, Y.: Negative aerosol-cloud re relationship from aircraft observations over Hebei, China. *Earth and Space Science*, 5, 19-29, 2018.
- Zhang, X. L., Zhao, Y.: Identification of the driving factors' influences on regional energy-related carbon emissions in China based on geographical detector method. *Environ. Sci. Pollut. Res.* 25, 9626-9635, 2018.
- 1290 Zhou, C. S., Chen, J., Wang, S. J.: Examining the effects of socioeconomic development on fine particulate matter (PM<sub>2.5</sub>) in China's cities using spatial regression and the geographical detector technique. *Sci. Total Environ.* 619, 436-445, 2018.

~~Yuan, T., Li, Z., Zhang, R., and Fan, J.: Increase of cloud droplet size with aerosol optical depth: an observation and modeling study, J. Geophys. Res., 113, D04201, doi:10.1029/2007JD008632, 2008.~~